ARMY RESEARCH LABORATORY

Investigation of Transition Metal Oxides with the Perovskite Structure as Potential Multiferroics

by Virginia Lea Miller and Steven C. Tidrow

ARL-TR-4621 **October 2008**

NOTICES

Disclaimers

The findings in this report are not to be construed as an official Department of the Army position unless so designated by other authorized documents.

Citation of manufacturer's or trade names does not constitute an official endorsement or approval of the use thereof.

Destroy this report when it is no longer needed. Do not return it to the originator.

Army Research Laboratory
Adelphi, MD 20783-1197

ARL-TR-4621 **October 2008**

Investigation of Transition Metal Oxides with the Perovskite Structure as Potential Multiferroics

Virginia Lea Miller and Steven C. Tidrow
Sensors and Electron Devices Directorate, ARL

REPORT DOCUMENTATION PAGE

Form Approved
OMB No. 0704-0188

1. REPORT DATE *(DD-MM-YYYY)*	2. REPORT TYPE	3. DATES COVERED (From - To)
October 2008	Summary	April 2006 to April 2007

4. TITLE AND SUBTITLE
Investigation of Transition Metal Oxides with the Perovskite Structure as Potential Multiferroics

5a. CONTRACT NUMBER

5b. GRANT NUMBER

5c. PROGRAM ELEMENT NUMBER

6. AUTHOR(S)
Virginia Lea Miller and Steven C. Tidrow

5d. PROJECT NUMBER

5e. TASK NUMBER

5f. WORK UNIT NUMBER

7. PERFORMING ORGANIZATION NAME(S) AND ADDRESS(ES)
U.S. Army Research Laboratory
ATTN: AMSRD-ARL-SE-RE
2800 Powder Mill Road
Adelphi, MD 20783-1197

8. PERFORMING ORGANIZATION REPORT NUMBER
ARL-TR-4621

9. SPONSORING/MONITORING AGENCY NAME(S) AND ADDRESS(ES)

10. SPONSOR/MONITOR'S ACRONYM(S)

11. SPONSOR/MONITOR'S REPORT NUMBER(S)

12. DISTRIBUTION/AVAILABILITY STATEMENT
Approved for public release; distribution unlimited.

13. SUPPLEMENTARY NOTES

14. ABSTRACT
Materials that exhibit both magnetism and ferroelectricity are often termed magnetoelectric multiferroics and are of recent interest because of their potential use in various microelectronic devices. There are many oxides that crystallize in the perovskite structure (ABO_3) which are either ferromagnetic or ferroelectric, but relatively few that display both types of properties. This research effort focused on transition metal oxides that crystallize in the perovskite structure as a potential source of multiferroic materials. All materials were prepared as bulk polycrystalline compounds using traditional solid state chemistry techniques. Various concentrations of magnetic atoms (such as Co^{2+}, Fe^{3+}, Cr^{3+}, Mn^{2+}) were substituted into a ferroelectric compound (mainly $BaTiO_3$) in an attempt to induce a magnetic moment in the material without destroying its ferroelectric properties. A solid solution was found to exist between $BaTiO_3$ and $LaFeO_3$, which is an antiferromagnetic oxide with the perovskite structure. Several compounds along this solid solution were also synthesized and characterize in an attempt to locate a novel material that displays the properties of both end members.

15. SUBJECT TERMS
Multiferroics, perovskite, transition metal oxides

16. SECURITY CLASSIFICATION OF:			17. LIMITATION OF ABSTRACT	18. NUMBER OF PAGES	19a. NAME OF RESPONSIBLE PERSON
a. REPORT	b. ABSTRACT	c. THIS PAGE			Robert Reams
U	U	U	UU	40	19b. TELEPHONE NUMBER (*Include area code*) 301-394-2800

Standard Form 298 (Rev. 8/98)
Prescribed by ANSI Std. Z39.18

Contents

List of Figures

List of Tables

Acknowledgments

This work was funded by the National Research Council's Research Associateship Program. Dr. V. Miller would like to thank Dr. Greg Fischer from the U.S. Army Research Laboratory for performing the magnetic measurements and Mr. Bernard Rod, also from the U.S. Army Research Laboratory, for his assistance in depositing metal contacts on the samples.

1. Introduction

Multiferroic materials are intriguing because of the coexistence of two or three of the following properties: ferromagnetism, ferroelectricity, and ferroelasticity (*1*). These three states are "switchable" in that they can be controlled by the application of a magnetic or electric field (*2,3*). Materials that exhibit both magnetism and ferroelectricity are often termed magnetoelectric multiferroics and are of recent interest because of their potential uses in various microelectronic devices (*2 through 8*). For example, in electronic storage devices the data is stored as regions of opposite magnetic alignment in ferromagnets. Ferroelectrics, on the other hand, are used widely as sensors. Since ferroelectrics are also ferroelastics, they are used in sonar detectors to convert sound waves into electrical signals and they are used in actuators to convert electrical impulses into motion. In multiferroic materials, the magnetic moments can be manipulated by an applied electric field, and the electric domains can be switched by an applied magnetic field (*1*). This leads to the possibility of designing new devices such as electric field controlled magnetic data storage, transducers that can convert between magnetic and electric fields and electric field controlled ferromagnetic resonance devices.

However, compounds that exhibit a coupling of magnetism and ferroelectricity are extremely rare. This is mainly attributed to the presence of transition metal *d* electrons, which are essential for magnetism, but hinder the tendency for off-center structural distortions which are necessary for ferroelectricity (*2*). In a ferromagnetic material, the spins of the unpaired *d* electrons align parallel in the presence of an applied magnetic field resulting in an observed magnetic moment. The driving force for this phenomenon is the exchange energy, which is minimized when all the unpaired electrons have the same spin state. This exchange energy dominates over the band energy only in narrow bands, such as those arising from the *d* orbitals of transition metals, which have a high density of states at the Fermi energy. Therefore, ferromagnetism arises in materials that contain atoms with unpaired electrons, such as Fe^{3+} and Mn^{2+}, which corresponds to partly filled *d* orbitals. Ferroelectricity occurs when all of the individual dipoles within a material align themselves parallel in an electric field. The resulting polarization can be manipulated by an externally applied electric field. Unlike ferromagnets, most ferroelectrics are composed of transition metals that have completely filled or completely empty *d* orbitals such as Ti^{4+} and Ta^{5+} (d^0 ions). A critical requirement for ferroelectricity is the absence of a center of symmetry in the crystal structure. For example, $BaTiO_3$ has a cubic (centrosymmetric) perovskite structure above 408K (135 °C) and does not possess a net dipole. Below 408K, a structural distortion occurs, and the Ti atom is displaced slightly from its central position within the TiO_6 octahedra to yield a noncentrosymmetric tetragonal structure. This off-centering is stabilized by a charge transfer from the filled oxygen *2p* orbitals to the *d* orbitals of the transition metal. This can only occur if the *d* orbitals are empty.

Although rare, there are several compounds that are known to exhibit magnetism and ferroelectricity and some even exhibit a coupling between the two. This coupling is often manifested as a change in the dielectric constant at the magnetic ordering temperature or a change in magnetization at the ferroelectric Curie temperature. One of the best known multiferroic materials is $BiFeO_3$ which is G-type antiferromagnet ($T_N \sim 643K$) and a ferroelectric ($T_c \sim 1103K$, polarization of 6.1 $\mu C/cm^2$ along the (111) direction at 77K) (*9*). It has a rhombohedrally distorted perovskite structure (space group R3c) and it exhibits weak magnetism at room temperature due to a canted spin structure. The ferroelectric properties are the result of a structural distortion driven by the Bi ion, which is highly polarizable due to the presence of the $6s^2$ lone pair (*9,10,11*). Epitaxial thin films of $BiFeO_3$ ranging from 50-500 nm have been grown on a $SrTiO_3$ substrate using pulsed laser deposition (*12*). These thin films exhibit a room temperature polarization of 50-60 $\mu C/cm^2$, which is much larger than that observed in the bulk material. This result was attributed to the high sensitivity of the polarization to small changes in the lattice parameters. Whereas bulk $BiFeO_3$ has a rhombohedral structure, $BiFeO_3$ thin films were found to have a monoclinic structure (*12*). Moreover, these thin films exhibited a thickness-dependant magnetization. The saturation magnetization decreased from 1 μ_B per unit cell for a 70 nm thick film to 0.O3 μ_B per unit cell for a 400 nm thick film (*12*).

Another multiferroic compound is $YMnO_3$, which is a hexagonal perovskite (space group $P6_3cm$) that is ferroelectric ($T_c \sim 950K$) and antiferromagnetic ($T_N \sim 76K$) (*13 through 17*). In this compound, the Mn^{3+} ion is not located in the center of an O_6 octahedral (as is the case in an ideal perovskite). Rather, it is located in the center of an O_5 trigonal biprism (*13*). A superexchange mechanism occurs between the adjacent Mn^{3+} ions and leads to antiferromagnetic behavior. The ferroelectric polarization is believed to be caused by the buckling of the MnO_5 polyhedral accompanied by the displacement of the Y ions (*13*). The crystal field produced by this distortion results in an ordering of the *d* orbitals in which the d_z^2 orbital is left unoccupied. This d_z^2 orbital is then able to hybridize with the oxygen $2p_z$ orbital resulting in the presence of ferroelectricity along the *c-axis.* This compound has a spontaneous polarization of ~5.5 $\mu C/cm^2$. $BiMnO_3$ is both ferromagnetic and ferroelectric (*17 through 21*). It is a high pressure phase that is synthesized at 3 GPa. At room temperature it has a monoclinic structure (space group. C2), which changes to orthorhombic (s.g. Pbnm) at the ferroelectric transition temperature of ~760K. Ferromagnetic ordering occurs below 105K and the material has a saturation magnetization of 3.6 μ_B per formula unit. Multiferroic behavior had been observed at ~80K with a magnetization of ~1 μ_B per Mn atom and a polarization of < 0.15 $\mu C/cm^2$. A change of ~0.6% in the dielectric constant was recorded at the ferromagnetic temperature under the application of an applied magnetic field of 8 Tesla. It is postulated that the Bi ions plays a role is stabilizing the ferromagnetism and inducing the ferroelectric distortion (*17*).

$EuTiO_3$ also exhibits some potentially interesting multiferroic properties (*22*). The compound has a simple cubic perovskite structure and is defined as a quantum paraelectric. It consists of Eu^{2+} ions with a spin of 7/2 and it has an antiferromagnetic ordering temperature of ~5.5K (*22*).

Measurements reveal that the dielectric constant decreases at the magnetic ordering temperature and the dielectric constant changes by about 7% under the application of a 1.5 Tesla field (*22*). Additional studies are needed. However, the preliminary results indicate a strong coupling between the Eu^{2+} spins and the dielectric constant.

The high-pressure (6 GPa) compound Bi_2NiMnO_6 is a heavily distorted double perovskite with the Ni^{2+} and Mn^{4+} ions ordered in a rock salt configuration. The compound is reported to be ferromagnetic with an ordering temperature of 140K and ferroelectric with a T_c of 485K (*23*). The ferroelectricity is proposed to arise from the presence of $6s^2$ lone pairs of Bi^{3+} ions and the ferromagnetism is a result of magnetism from the Ni^{2+} and Mn^{4+} ions. The dielectric constant changed by about 0.4% at 140K and 10 kHz and an applied field of 9 Tesla (*23*).

$CdCr_2S_4$, which has the spinel structure, was recently reported to be a low temperature multiferroic (*24*). In this compound, the Cr^{3+} ions are octahedrally surrounded by S ions which results in a half-filled lower t_{2g} state with a spin of 3/2. The material is ferromagnetic with a T_c of ~100K and it exhibits soft magnetic behavior with a saturation magnetization of 3 μ_B per Cr^{3+} (*24*). The magnetization is believe to arise from a superexchange mechanism between Cr^{3+} ions. Plots of the dielectric constant versus temperature at various frequencies reveals that $CdCr_2S_4$ acts as a relaxor ferroelectric below 135K with a polarization of 0.5 $\mu C/cm^2$ (*24*). The dielectric constant also exhibits a steep rise below the ferromagnetic transition temperature and this change is believed to be driven by the onset of magnetic ordering. Since both the ferromagnetic and ferroelectric properties are believed to be linked to the Cr^{3+} ions, this materials could prove to be a very interesting and potentially useful multiferroic.

The compound $TbMn_2O_5$ has also shown some interesting multiferroic behavior (*25,26*). This compound is orthorhombic (space group Pbam) at room temperature and contains both Mn^{4+} and Mn^{3+} ions. The Mn^{4+} ions are octahedrally coordinated by oxygen, whereas the Mn^{3+} ions are located at the base center of a square pyramid. Long range antiferromagnetic ordering of the Mn ions occurs at 40K with a spin reorientation at ~25K. The ordering of the Tb^{3+} ions is suspected to occur around 10K. The onset of ferroelectricity was seen at 38K with a dominant polarization along the *b*-axis. Since the magnetic and ferroelectric ordering temperatures are so similar, Hur et al., have postulated that the long range ordering of the Mn^{4+}/Mn^{3+} ions induces the ferroelectric transition (*25*). This is believed to occur by inducing an additional distortion of the Jahn-Teller-distorted Mn^{3+} neighbors. Moreover, Hur et al., have shown that the dielectric constant along the b-axis can be strongly influenced by an applied magnetic field and they have been able to reversibly switch the electric polarization of $TbMn_2O_5$ using a magnetic field of 0-2 Tesla (*25*).

Ab initio calculations have be used to predict the coexistence of ferromagnetism and ferroelectricity is the double perovskite Bh_2FeCrO_6 (*27*). In this scenario, the ferroelectricity is due to the $6s^2$ lone pair on the Bi whereas the ferromagnetism arises from a ferrimagnetic interaction between the Cr^{3+} and Fe^{3+} ions. This compound was predicted to have a

polarization of ~80 $\mu C/cm^2$ and a magnetization of ~2 μ_B per formula unit (*27*). First-principle density functional calculations performed on $BiCrO_3$ indicate that its structure is pseudo-triclinic (*28*). It is predicted to be antiferromagnetic and not ferroelectric due to the fact that the Cr^{3+} ion appears to resist an off-center distortion (*28*).

Another approach to the search for novel multiferroic materials is through the design of multiphase materials, such as composites or multilayer thin films that consist of a ferromagnetic material and a ferroelectric material. In this scenario, a coupling between the two properties is a results of the strain induced on one of the materials by the other. Large surface areas are need to see a large effect, therefore these materials are typically prepared as thin films. For example, nanopillars of $CoFe_2O_4$ (a compound with the spinel structure) grown in a $BaTiO_3$ (perovskite structure) matrix have shown multiferroic behavior (*29*). In this material, the $BaTiO_3$ is responsible for producing the ferroelectricity whereas the magnetism comes from the $CoFe_2O_4$. Measurements indicate a coupling between the two phenomenon and this coupling is manifested as a change in the magnetization of about 5% at the ferroelectric Curie Temperature (390K) (*29*).

Thin films of a superlattice composed of ferromagnetic $La_{0.7}Ca_{0.3}MnO_3$ and ferroelectric $BaTiO_3$, which were grown on $SrTiO_3$ substrates, have also been shown to display magnetoelectric properties (*30*). These films were ferromagnetic at temperature between 145K and 158K and were ferroelectric at temperature ranging from 55-105K depending on the Ba content (*30*). The films were found to be multiferroic when measurements revealed the presence of a negative magnetocapacitance, which reaches a maximum at the ferroelectric transition temperature.

One potential source of multiferroic materials are compounds that crystallize with the perovskite structure, ABX_3 (where X can be O, F, CI or sometimes Br). There are many oxides that crystallize in the perovskite structure (ABO_3) that are either magnetic or ferroelectric, but only a few, such as $YMnO_3$, $BiFeO_3$ and $BiMn\ O_3$, that exhibit both properties. The perovskite crystal structure is one of the most commonly encountered structures in solid-state chemistry. It consists of comer sharing BO_6 octahedra with the A cations (large purple sphere) located in the 12-fold coordination site between these octahedra (figure 1) (*31*).

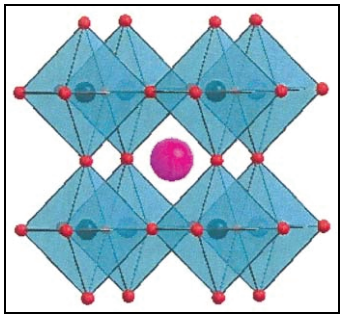

Figure 1. The ideal cubic perovskite structure.

Many ternary compounds, especially oxides, form a simple perovskite structure. However, more complicated variations, such as mixing of atoms on the B site ($ABB'X_3$) or vacancies on the X site (ABX_{3-y}) are also found to occur. This structure is extremely flexible and it can accommodate almost all of the elements in the periodic table (*31,32*). Often the A and B cations are not exactly the right size to fit into the sites generated by this structure. As a result, the structure is easily distorted from its ideal cubic symmetry to lower symmetries depending on the elements present. The Goldsmith tolerance factor (t) is often used to predict whether a compound will form the perovskite structure and it is given by:

$$t = \frac{R_A + R_O}{\sqrt{2(R_B + R_O)}}$$

where R_A is the radius of the A ion, R_B is the radius of the B ion and R_O is the radius of O^{2-}. A cubic perovskite usually forms when t is in the range $0.9 < t < 1$. For $t >> 1$, the B cation is too small to occupy the B site and the structure changes completely. For smaller values of t ($0.85 < t < 0.9$), the structure distorts to accommodate the smaller A cation (i.e., the framework of octahedra twists or distorts slightly). For $t < 0.85$, the distorted perovskite is not stable and the structure changes completely. It is common in most ternary oxides that the introduction of smaller A-site cations causes the BO_6 octahedra to "tilt". This tilting causes the BO_6 octahedra to distort such that the B-O-B bonds are no longer equal to 180°. As a result, the symmetry of the structure is reduced. This is illustrated in the A_2FeMoO_6 (A=Ba, Sr or Ca) perovskite series (*33*). Ba_2FeMoO_6 is a cubic perovskite. The presence of Sr (which is smaller than Ba) on the A-site leads to tetragonal symmetry. And when Ca is introduced onto the A-site, the symmetry is further reduced, resulting in a monoclinic unit cell (*33*). Numerous types of octahedra titling are possible and the tilt system is typically described in terms of the BO_6 rotation about any of the three Cartesian axes, (x,y,z) (*34*). The resulting tilt angles are most accurately obtained from structural data, mainly atomic coordinates. Because of the intimate relationship between crystal structure and properties, these structural distortions often result in variations in the physical properties. For example, Colla *et al.,* have observed a correlation between the occurrence of octahedra tilting and the temperature coefficient of resonant frequency in the $Sr(Zn_{1/3}NbY)O_3$-$Ba(Zn_{1/3}Nb_{2/3})O_3$ solid solution (*35*). And recently, Lufaso *et al.,* have reported that the dielectric properties of several $Ba_3MM'_2O_9$ (M=Mg, Ni, Zn; M'=Nb, Ta) perovskites can be correlated to differences in atomic coordination environments (*36*).

In addition to being numerous in nature, perovskite materials exhibit a wide range of physical properties. Some examples include $CaTiO_3$, which is a dielectric, $BaTiO_3$, a ferroelectric, $Pb(Zr_{1-x}Tix)O_3$, a piezoelectric, $(Y_{1/3}Ba_{2/3})CuO_{3-x}$, a high temperature superconductor, and the $AMnO_3$ (A=Ca, Sr, Ba) family of compounds which exhibits giant magnetoresistance (*32*). Perovskite materials are also used as semiconductors, insulators, catalysts, thermoelectrics, pyroelectrics and in optical and electro-optic devices (*34*). The substitution of different cations into the metal-oxygen octahedra leads to a large class of compounds known as double

perovskites, or $A_2BB''O_6$. Substitutions can also be made on the A-site yielding $AA'BB''O_6$ type compounds. Because of the various combinations of A, A', B and B" cations that are possible, these compounds have the potential to exhibit a combination of different physical properties.

The focus of this research has been to study compounds with the double perovskite structure as potential multiferroic materials. Perovskites typically have large internal fields which are necessary for the presence of ferroelectricity (*16*). Also, the B-O-B bond angle is equal to or near 180°, which allows for the possibly of indirect superexchange interactions resulting in magnetic ordering in the B lattice. The objective of this research effort was to introduce various concentrations of magnetic atoms, such as Fe^{3+}, Cr^{3+}, Co^{2+} and Mn^{3+}, into a ferroelectric material (mainly $BaTiO_3$) in an attempt to induce magnetism without destroying the ferroelectric property. Various lanthanides (such as La^{3+} and Nd^{3+}) were substituted onto the A-site to ensure charge neutrality.

2. Experimental Methods

Polycrystalline samples were prepared by traditional solid state chemistry techniques. Stoichiometric amounts of binary oxides were mixed together with ethanol and then pressed into pellets with a diameter of 11 mm and a thickness of 4.5 mm. All reagents had a purity of 99.9% or better. La_2O_3 was dried at 900 °C immediately prior to weighing. The pellets were calcined at 900 °C for 12 hours, then reground, pressed into pellets, and placed on sacrificial powder of the sample composition on Pt foil on an alumina slab. The pellets were then heated at a rate of 3 °C/min to 1350 °C for 36-48 hours and then quenched in the furnace.

Phase purity was determined by powder X-ray diffraction using a Rigaku Ultima Powder X-Ray Diffractometer. Diffraction patterns were collected at room temperature using CuKα radiation. Scans were run between 5 and 60° 2θ with a 0.02° 2θ step size.

E-beam evaporation techniques were used to deposit contacts on circular samples of ~10.5 mm diameter and 0.5 mm thickness to form a parallel plate capacitor. The contacts were composed of layers of 250Å Ti, 1500Å Au, 3000Å Ag, and 1500Å Au in that order. The small-signal capacitance was measured by an impedance bridge in the temperature range $-55 \le T \le 120$ °C and the frequency range $0 \le f \le 1\times10^6$ Hz at 5 values of bias voltage across the capacitors from 0 to 500 V. The bias voltages needed for the measurement are provided by a Bertan 205B high-voltage D.C. power supply.

Magnetic hysteresis loops were measured between –1.25 Tesla and 1.25 Tesla at 25 °C.

3. Results and Discussion

General Analysis and Results

Table 1 presents a list of single-phase samples that were prepared via the experimental method described above. All of these materials were found to have the perovskite structure. The color of the samples ranged from yellow (for the Cr-containing compounds) to dark brown (for the Fe-containing compounds) to black for the Mn-containing compounds. The X-ray diffraction patterns could be indexed using a cubic unit cell and the space group Pm-3m (modeled after $SrTiO_3$). The lattice constants were calculated using the following method:

In a cubic system:

$$\frac{\Delta d}{d} = \frac{\Delta a}{a} = \frac{a - a_o}{a_o} = \mathrm{K}[(\cos^2\theta/\sin\theta) + (\cos^2\theta/\theta)]$$

where d is the interplanar spacing, a is the calculated unit cell parameter, a_o is the true value of the cell parameter and K is a constant. The term in the brackets is called the Nelson-Riley Function and the value of a_o can be found by plotting a against this function, which approaches zero as θ approaches 90 °C. The value of a in a cubic system can be calculated using the following equation:

$$\mathrm{a}^2 = d^2(\mathrm{h}^2 + \mathrm{k}^2 + \mathrm{l}^2)$$

where h, k and l are the Miller indices corresponding to each value of d. The Goldsmith tolerance factor was also calculated for each sample and in many samples, the tolerance factor was calculated to be slightly greater than 1. The cubic lattice parameter, a, for each sample was predicted using the following formula and was then compared to the actual lattice parameter obtained from the X-ray diffraction data:

$$a_{\mathrm{pred}} = \frac{(\mathrm{R_A} + \mathrm{R_O})}{\sqrt{2}} + \mathrm{R_B} + \mathrm{R_O}$$

where R_A is the radius of the A ion, R_B is the radius of the B ion and R_O is the radius of O^{2-}. The Clausius-Mossotti Relation was used to predict the dielectric constant (ε) of each sample using the molar volume calculated from the *actual* cubic lattice parameter. The Clausius-Mossotti relationship is given by the equation:

$$\varepsilon = \frac{3\mathrm{V_m} + 8\pi\alpha_\mathrm{T}}{3\mathrm{V_m} - 4\pi\alpha_\mathrm{T}}$$

where V_m is the molar volume of the compound (in $Å^3$) and α_T is the total polarizability (in $Å^3$) of the substance. The polarizability follows the additivity rule so the total polarizability for a compound such as $BaTiO_3$ could be written as:

$$\alpha_T(BaTiO_3) = \alpha(Ba) + \alpha(Ti) + 3\alpha(O)$$

where $\alpha(Ba)$, $\alpha(Ti)$, and $\alpha(O)$ are the polarizabilities of the Ba^{2+}, Ti^{4+} and O^{2-} ions respectively. The results for a select list of single phase compounds are presented in table 1. The tolerance factor and the cubic unit cell parameter were not calculated for compounds containing Nd^{3+} on the A-site because of the lack of data on the size of an Nd^{3+} ion in a 12-fold coordination site. Table 2 lists additional sample compositions that were attempted but resulted in multiphase products.

Table 1. List of single phase compounds.

Compound	Tolerance Factor	Theoretical a (Å) (if cubic)	Actual a (Å) (if cubic)	Polarizability (Å^3)	Predicted Molar Volume (Å^3)	Actual Molar Volume (Å^3)	Predicted Dielectric Constant
$La_2Ba(Fe_2Ti)O_9$	1.01	3.96	3.95	14.713	61.96	61.62	–19000
$La_2Ba(Fe_{1.75}A_{10.25})TiO_9$	1.01	3.95	3.93	14.588	61.86	60.70	–450
$(LaNd)BaFe_2TiO_9$			3.93	14.36		60.69	300
$Nd_2BaFe_2TiO_9$			3.92	14.007		60.24	100
$La_2Ba(Mn_2Ti)O_9$	1.00	3.98	3.94	14.946	63.04	61.16	–130
$(LaNd)BaMn_2TiO_9$			3.93	14.593		60.69	–420
$La_2Ba(Co_2Ti)O_9$	1.01	3.95	3.89	14.286	61.82	58.86	–182
$La_2Ba(Fe_2Sn)O_0$	0.996	3.99	3.99	14.68	63.33	63.52	90
$La_2Ba_2(Fe_2Nb)O_9$	1.03	4.03	4.02	15.17	65.69	64.96	135
$LaBa_2(Fe_2Ta)O_9$	1.03	4.03	4.01	15.423	65.69	64.48	–1565
$LaBa_2(FeTi_2)O_9$	1.03	4.04	3.97	15.036	65.94	62.57	–450
$LaBa_2(MnTi_2)O_9$	1.03	4.05	3.97	15.153	66.43	62.57	–200
$LaBa_2(CrTi_2)O_9$	1.02	4.06	3.96	14.756	66.92	62.10	640
$LaBa_2(Fe_{1/4}Dr_{3/4})Ti_2O_9$	1.03	4.06	3.96	14.826	66.92	62.10	–62000
$NdBa_2(Fe_{1/4}Cr_{3/4})Ti_2O_9$	1.00	4.00	3.95	14.473	64.00	61.63	200
$Ba_2La(Al_{1/4}Cr_{3/4})Ti_2O_9$	1.03	4.06	3.95	14.702	66.92	61.63	4000
$Ba_2La(Fe_{0.5}Cr_{0.5})Ti_2O_9$	1.03	4.05	3.96	14.897	66.43	62.10	–600
$Ba_2La(Fe_{3/4}Cr_{1/4})Ti_2O_9$	1.03	4.05	3.97	14.967	66.43	62.57	–1500
Ba_2CoTaO_6	1.07	4.1	4.07	15.62	68.92	67.42	100
Ba_2CoNbO_6	1.07	4.1	4.07	15.24	68.92	67.42	55
$Ba_3CuTa_2O_9$	1.02	4.19	Not cubic	16.286	73.56	Not cubic	—
$Sr_3CuNb_2O_9$	0.97	4.08	Not cubic	13.62	67.92	Not cubic	—
$Sr_3CuTa_2O_9$	0.97	4.08	Not cubic	14.126	67.92	Not cubic	—

Table 1. List of single phase compounds (continued).

Compound	Tolerance Factor	Theoretical a (Å) (if cubic)	Actual a (Å) (if cubic)	Polarizability (Å^3)	Predicted Molar Volume (Å^3)	Actual Molar Volume (Å^3)	Predicted Dielectric Constant
$Ba(FeTa)_{0.15}Ti_{0.7}O_3$	1.05	4.12	4.02	15.534	69.93	64.96	–1700
$Ba(CoW)_{0.15}Ti_{0.7}O_3$	1.06	4.13	4.02		70.44		
$Ba_{0.8}La_{0.2}(FeMn)_{0.1}Ti_{0.8}O_3$	1.04	4.08	3.98	15.201	67.92	63.04	- –300
$Ba_{0.8}La_{0.2}(FeCr)_{0.1}Ti_{0.8}O_3$	1.04	4.08	3.97	15.082	67.92	62.57	–300
$Ba_{0.6}La_{0.4}(FeCr)_{0.2}Ti_{0.6}O_3$	1.02	4.04	3.96	14.804	65.94	62.099	2000
$Ba_{0.85}La_{0.15}Fe_{0.15}Ti_{0.85}O_3$	1.05	4.09	3.99	15.214	68.42	63.52	–900
$Ba_{0.85}La_{0.15}Cr_{0.15}Ti_{0.85}O_3$	1.04	4.10	3.98	15.088	68.42	63.04	–1200

Table 2. List of multi-phase samples.

Compound	Tolerance Factor	Theoretical *a* (Å)	Estimated Molar Volume (Å^3)	Polarizability (Å^3)	Estimated Dielectric Constant (ε)
La_2CoTiO_6	0.946	3.95	61.63	14.39	134
La_2CoZrO_6	0.922	4.01	84.48	14.55	53
La_2NiTiO_6	0.937	3.98	63.04	14.18	50
La_2NiZrO_6	0.911	4.03	65.45	14.34	34
La_2MnTiO_6	0.944	3.96	62.1	14.885	–750
La_2MnZrO_6	0.918	4.02	64.96	15.045	100
La_2MnSnO_6	0.924	4.00	64.00	14.835	100
La_2CoSnO_6	0.929	3.99	63.52	14.34	51
La_2NiSnO_6	0.918	4.02	64.96	14.13	32
$La_2Ba(Fe_2Zr)O_9$	0.991	4.02	64.96	14.82	65
$La_2Ba(Cr_2Zr)O_9$	0.970	4.06	66.92	14.26	25
$La_2Ba(Co_2Zr)O_9$	0.999	4.01	64.48	14.393	44
$La_2Ba(Cr_2Ti)O_9$	0.989	4.00	64.00	14.153	40
$LaBa_2(Mn_{0.2}Cr_{0.8})Ti_2O_9$	1.02	4.06	66.92	14.836	40
$LaBa_2CoTi_2O_9$	1.04	4.03	65.45	14.823	56
$Ba_2La(CO_{0.25}Cr_{0.75})Ti_2O_9$	1.03	4.06	66.92	14.773	38

Substitution of Fe^{3+} into $BaTiO_3$

Attempts were made to substitute Fe^{3+} (a magnetic atom) for Ti^{4+} (a nonmagnetic atom) in $BaTiO_3$ in hopes of inducing magnetism without destroying the ferroelectricity of the material. In order to ensure charge neutrality, La^{3+} was substituted for Ba^{2+} to yield compounds with the general formula $Ba_{l-x}La_x(Ti_{l-x}Fe_x)O_3$ where x=0.l5, 0.33 and 0.66. The x=0.33 compound can be rewritten as $Ba_2La(Ti_2Fe)O_9$ and the x=0.66 compound can be rewritten as $BaLa_2(TiFe_2)O_9$. These compounds can also be described as a solid solution between $BaTiO_3$, which is a ferroelectric perovskite, and $LaFeO_3$, which is an antiferromagnetic perovskite ($T_N \sim 740K$). Table 3 lists the tolerance factor, sample color and cubic unit cell parameter for each of the prepared compounds. Table 4 lists the predicted dielectric constant of each compound as well as the actual dielectric behavior. Figure 2 is the X-ray diffraction patterns of $Ba_{l-x}La_x(Ti_{1-x}Fe_x)O_3$ where x=0.15, 0.33 and 0.66. Figures 3, 4 and 5 are plots of the dielectric constant (at E=O) and percent tuning as a function of temperature and frequency for $Ba_{l-x}La_x(Ti_{1-x}Fe_x)O_3$ where x=0.15, 0.33 and 0.66 respectively. Figure 6 is a plot of the magnetic response (emu) as a function of applied magnetic field (Oe) for the x=0.15 compound. Figure 7 is a similar plot for the x=0.33 and x=0.66 compounds.

Table 3. Summary of $Ba_{l-x}La_x(Ti_{1-x}Fe_x)O_3$ compounds.

Compound	Tolerance Factor	Sample Color	Predicated *a* (Å)	Actual *a* (Å)	Polarizability (Å^3)	Actual Molar Volume (Å^3)
x=0.15	1.04	dull green	4.10	3.99	15.214	63.52
x=0.3 3	1.01	dark brown	4.06	3.97	15.036	62.57
x=0.66	1.01	dark brown	3.96	3.95	14.713	61.62

Table 4. Dielectric properties of the Bal_xLax(Til_xFex)O3 compounds.

Compound	Predicted Dielectric Constant (ε)	Measured Dielectric Properties
x=0.15	–900	ε increases continuously to 2500 at 120°C
x=0.33	–450	broad increase in ε with a maximum value of 30,000 at 80 °C
x=0.66	–-19000	no definitive peak

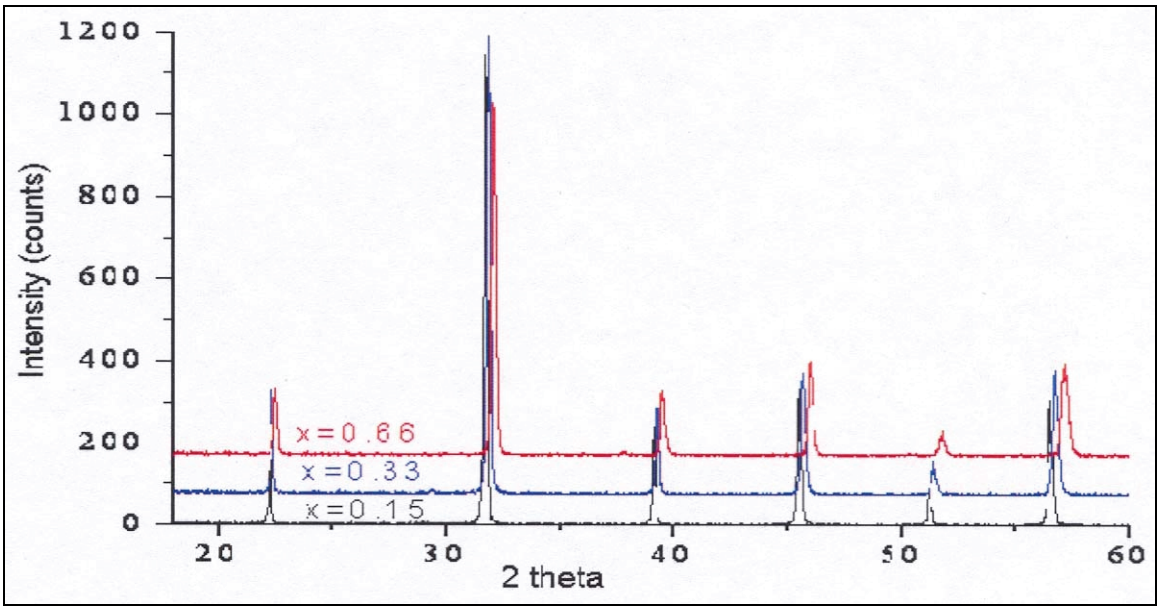

Figure 2. X-ray diffraction patterns of the $Ba_{1-x}La_x(Ti_{1-x}Fe_x)O_3$ compounds where x=0.15, 0.33 and 0.66.

All compounds were found to be single phase and range in color from dull green for $Ba_{0.85}La_{0.15}(Ti_{0.85}Fe_{0.15})O_3$ to dark brown for $Ba_{0.33}La_{0.66}(Ti_{0.33}Fe_{0.66})O_3$. These compounds were determined to have a tolerance factor around 1, indicating that they should crystallize with the perovksite structure. The X-ray diffraction patterns could be indexed using a cubic unit cell and space group Pm-3m (modeled after $SrTiO_3$). The unit cell parameter, *a*, varies from 3.99 Å for $Ba_{0.85}La_{0.15}(Ti_{0.85}Fe_{0.15})O_3$ to 3.95 Å for $Ba_{0.33}La_{0.66}(Ti_{0.33}Fe_{0.66})O_3$. As the concentration of Fe^{3+} increases, the unit cell parameter decreases. This is consistent with the fact that in a six-fold coordination environment the ionic radius of Fe^{3+} (0.55 Å for the low spin state) is less than the ionic radius of Ti^{4+} (0.605 Å). As a result, the substitution of Fe^{3+} for Ti^{4+} in this compound results in a smaller unit cell. More detailed structural studies need to be performed to determine ifthere is any ordering on the A- and/or B-site.

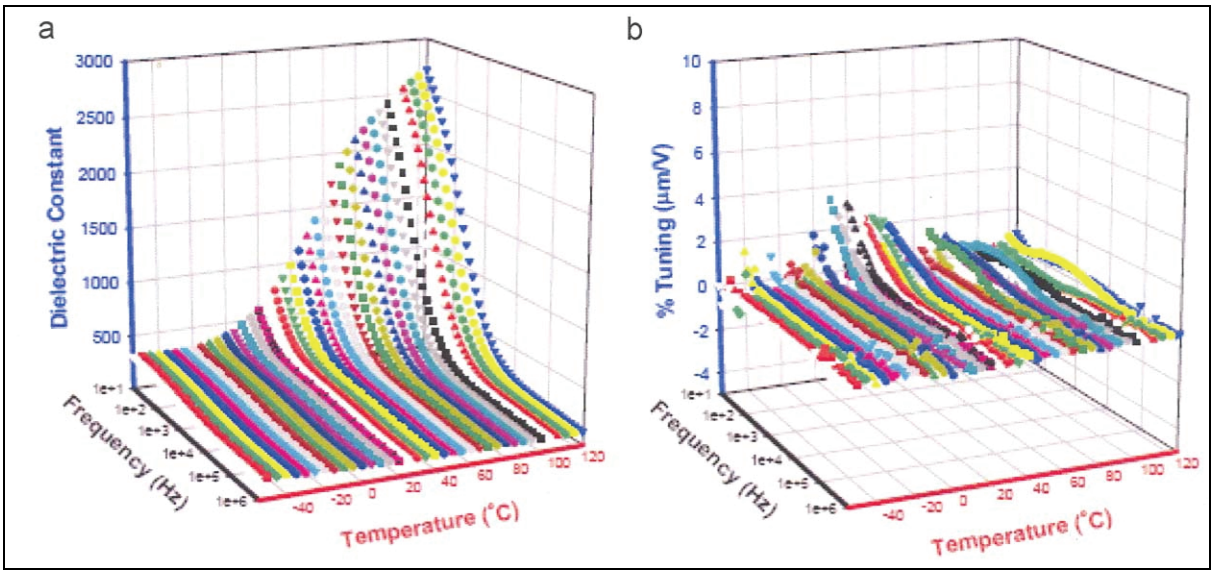

Figure 3. Dielectric constant at E=0 (a) and percent tuning (b) as a function of temperature and frequency for $Ba_{0.85}La_{0.15}(Ti_{0.85}Fe_{0.15})O_3$.

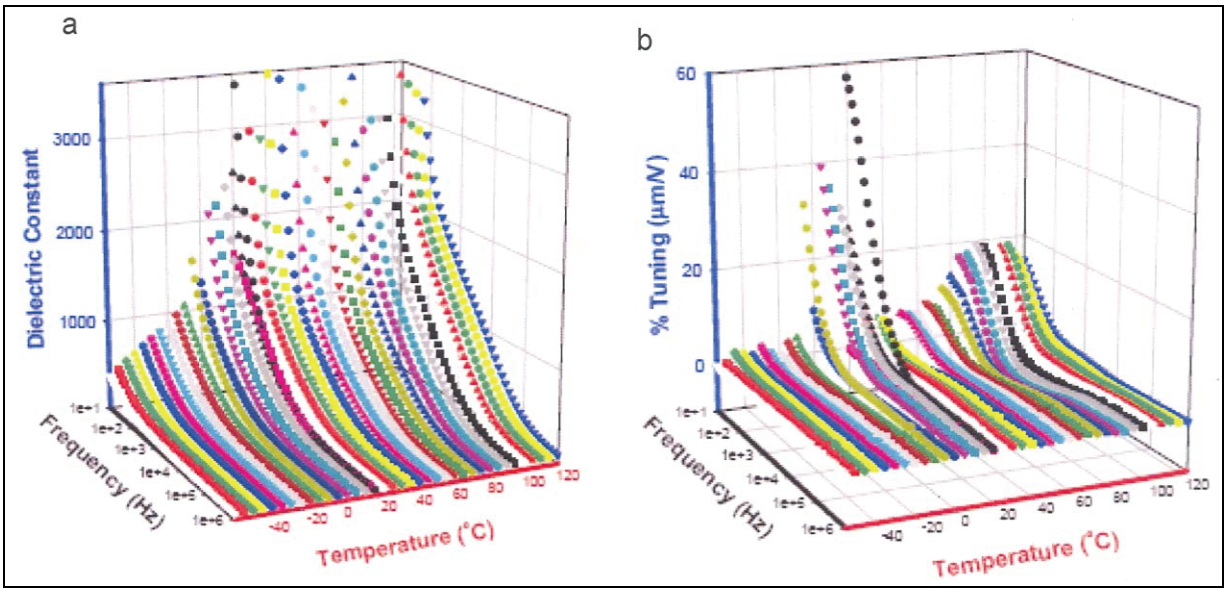

Figure 4. Dielectric constant at E=0 (a) and percent tuning (b) as a function of temperature and frequency for $Ba_{0.66}La_{0.33}(Ti_{0.66}Fe_{0.33})O_3$.

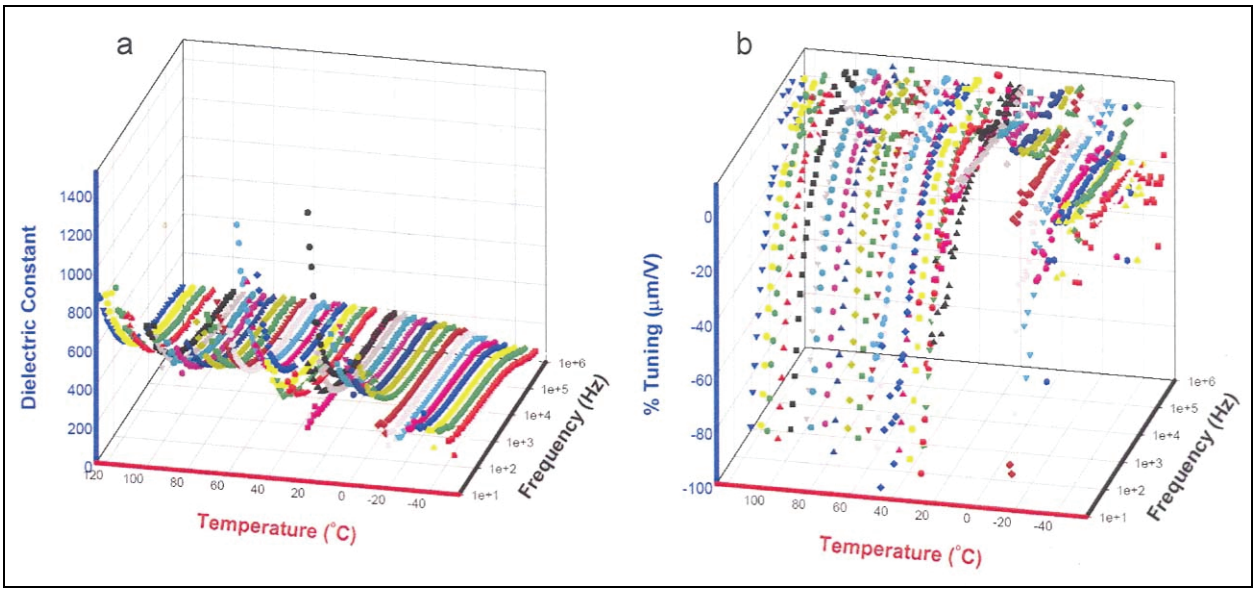

Figure 5. Dielectric constant at E=0 (a) and percent tuning (b) as a function of temperature and frequency for $Ba_{0.33}La_{0.66}(Ti_{0.33}Fe_{0.66})O_3$.

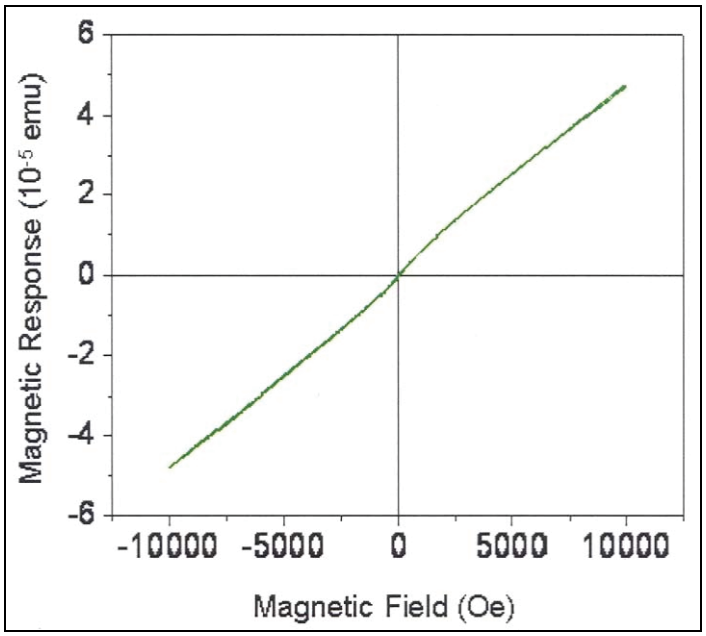

Figure 6. Magnetic response (emu) as a function of applied magnetic field (Oe) at 25 °C for $Ba_{0.85}La_{0.15}(Ti_{0.85}Fe_{0.15})O_3$.

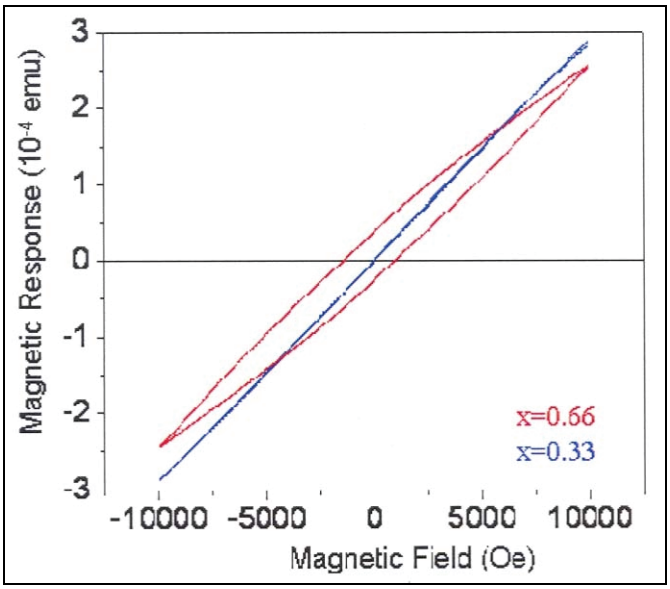

Figure 7. Magnetic response (emu) as a function of applied magnetic field (Oe) at 25 °C for $Ba_{0.85}La_{0.15}(Ti_{0.85}Fe_{0.15})O_3$ (x=0.33) and $Ba_{0.85}La_{0.15}(Ti_{0.85}Fe_{0.15})O_3$ (x=0.66).

Using the Clausius-Mossotti Relation, the dielectric constant of each compound was predicted. For all three compounds, a negative dielectric constant was calculated. This result indicates that these materials may be on the verge of a structural phase transition that may result in ferroelectric behavior. However, ferroelectricity was not observed in any of these compounds. For $Ba_{0.85}La_{0.15}(Ti_{0.85}Fe_{0.15})O_3$, the dielectric constant remains below 500 at temperatures below 20 °C. The dielectric constant then begins to increase to a value greater than 2500 as the temperature increases to 120 °C. This behavior is similar to that of $BaTiO_3$, which has a sharp peak in the dielectric constant at 130 °C corresponding to a tetragonal-cubic structural transition. It is possible that in $Ba_{0.85}La_{0.15}(Ti_{0.85}Fe_{0.15})O_3$ the small concentration of Fe^{3+} ions is causing a "broadening effect" in the ferroelectric properties of $BaTiO_3$. This effect only occurs at frequencies less than 1 kHz. Above 1 kHz, the dielectric constant has a value of 250 and is insensitive to temperature and frequency. This compound shows almost not tunability over the measured temperature and frequency range. Figure 6 reveals the magnetic properties of this compound. At 25 °C, $Ba_{0.85}La_{0.15}(Ti_{0.85}Fe_{0.15})O_3$ does not exhibit any magnetism in the presence of an applied magnetic field ranging from –1.25 Tesla to 1.25 Tesla. This compound appears to be paramagnetic at this temperature.

The dielectric constant of $Ba_{0.66}La_{0.33}(Ti_{0.66}Fe_{0.33})O_3$ has a very broad peak from 20 °C to 120 °C that reaches a maximum value of 30,000 (not shown in figure 4) at approximately 80 °C. This behavior is only seen at very low frequencies (less than 1 kHz). The compound also exhibits very little tunability. A maximum percent tuning occurs at temperatures above 80 °C and at frequencies less than 1 kHz. The magnetic properties of this compound are illustrated in figure 7. Similar to $Ba_{0.85}La_{0.15}(Ti_{0.85}Fe_{0.15})O_3$, $Ba_{0.66}La_{0.33}(Ti_{0.66}Fe_{0.33})O_3$ does not exhibit any

magnetism in the presence of an applied magnetic field ranging from –1.25 Tesla to 1.25 Tesla at 25 °C. This compound also appears to be paramagnetic at this temperature.

The dielectric properties of $Ba_{0.33}La_{0.66}(Ti_{0.33}Fe_{0.66})O_3$ are very intriguing. The dielectric constant does not show any unusual behavior as the temperature and frequency are varied. There are no discernable peaks in the plot and the dielectric constant never reaches values greater than 1000. This indicates that the ferroelectric properties of $BaTiO_3$ have been completely destroyed by the substitution of a high concentration of Fe^{3+} ions into the compound. However, this compound exhibits negative tunability (up to –80%) at low frequencies and no tunability at higher frequencies. The percent tuning was calculated from the following equation:

$$\%\,\text{tuning} = \frac{\varepsilon_{E=0} = \varepsilon_{E\neq 0}}{\text{electric field strength}}$$

where $\varepsilon_{E=0}$ is the dielectric constant in the absence of an applied electric field (E=0) and $\varepsilon_{E\neq 0}$ is the dielectric constant in the presence of an applied electric field (E≠0). In most cases, the percent tuning should be positive because the dielectric constant of a material typically decreases with increasing applied electric field. A negative percent tuning indicates that the dielectric constant is increasing as the electric field increases. This may be due to the fact that one or both of the B-site cations (either Fe^{3+} or Ti^{4+}) are shifting off-site towards the [111] direction. The B-site cation experiences a smaller local electric field in this direction because it does not encounter any other atoms in this direction. As a result, the repulsion forces between atoms are minimized and this may give rise to a higher dielectric constant in the material as the electric field is increased. The magnetic properties of $Ba_{0.33}La_{0.66}(Ti_{0.33}Fe_{0.66})O_3$ are revealed in figure 7. Unlike $Ba_{0.85}La_{0.l5}(Ti_{0.85}Fe_{0.33})O_3$ and $Ba_{0.66}La_{0.33}(Ti_{0.66}Fe_{0.33})O_3$, $Ba_{0.33}La_{0.66}(Ti_{0.33}Fe_{0.66})O_3$ exhibits a small magnetic hysteresis loop, which indicates the presence of a magnetic moment within the material. The magnetic data suggests that $Ba_{0.33}La_{0.66}(Ti_{0.33}Fe_{0.66})O_3$ is ferromagnetic at 25 °C.

Substitution of Cr^{3+} into $BaTiO_3$

Attempts were also made to substitute Cr^{3+} (a magnetic atom) for Ti^{4+} (a nomnagnetic atom) in $BaTiO_3$ in hopes of inducing magnetism without destroying the ferroelectricity of the material. In order to ensure charge neutrality, La^{3+} was substituted for Ba^{2+} to yield compounds with the general formula $Ba_{l-x}La_x(Ti_{l-x}Cr_x)O_3$ where x=0.15, 0.33 and 0.66. The x=0.33 compound can be rewritten as $Ba_2La(Ti_2Cr)O_9$ and the x=0.66 compound can be rewritten as $BaLa_2(TiCr_2)O_9$. These compounds can also be described as a solid solution between $BaTiO_3$, which is a ferroelectric perovskite, and $LaCrO_3$, which is an antiferromagnetic perovskite (T_N ~ 258K). Table 5 lists the tolerance factor, sample color and cubic unit cell parameter for each of the prepared compounds. Table 6 lists the predicted dielectric constant of each compound as well as the actual dielectric behavior. Figure 8 is the X-ray diffraction patterns of $Ba_{l-x}La_x(Ti_{l-x}Cr_x)O_3$ where x=0.15 and 0.33. The x=0.66 compound was found to be multi-phase. Figures 9

and 10 are plots of the dielectric constant (at E=O) and percent tuning as a function of temperature and frequency for $Ba_{1-x}La_x(Ti_{1-x}Cr_x)O_3$ where x=0.15 and 0.33 respectively. Figure 11 is a plot of the magnetic response (emu) as a function of applied magnetic field (Oe) at 25 °C for $Ba_{0.66}La_{0.33}(Ti_{0.66}Cr_{0.33})O_3$.

Table 5. Summary of $Ba_{1-x}La_x(Ti_{1-x}Cr_x)O_3$ compounds.

Compound	Tolerance Factor	Sample Color	Predicted *a* (Å)	Actual *a* (Å)	Polarizability (Å^3)	Actual Molar Volume (Å^3)
x=0.15	1.04	dull yellow	4.10	3.98	15.088	63.04
x=0.33	1.02	dark yellow	4.05	3.96	14.756	62.10
x=0.66	0.98	multi-phase	4.00	multi-phase	14.153	multi-phase

Table 6. Dielectric properties of the $Ba_{1-x}La_x(Ti_{1-x}Cr_x)O_3$ compounds.

Compound	Predicted Dielectric Constant (ε)	Measured Dielectric Properties
x=0.15	–1200	broad peak in ε with a maximum value of 2000 at 80 °C
x=0.33	640	extremely broad peak in ε with a maximum value of 1300 at 50 °C
x=0.66	40	not measured (material was multi-phase)

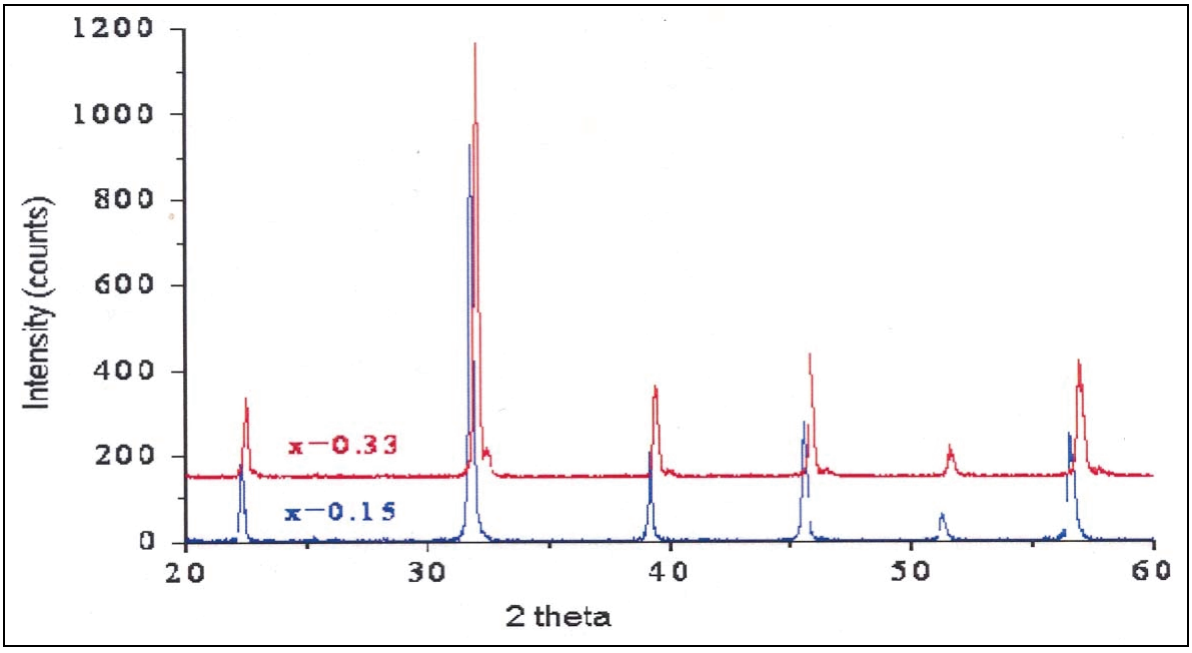

Figure 8. X-ray Diffraction patterns of the compounds $Ba_{1-x}La_x(Ti_{1-x}Cr_x)O_3$ where x=0.15 and 0.33. (The x=0.66 compound was found to be multi-phase.)

Both $Ba_{0.85}La_{0.15}(Ti_{0.85}Cr_{0.15})O_3$ and $Ba_{0.66}La_{0.33}(Ti_{0.66}Cr_{0.33})O_3$ were successfully prepared as single phase compounds. Both compounds have a yellowish color. Attempts to prepare $Ba_{0.33}La_{0.66}(Ti_{0.33}Cr_{0.66})O_3$ resulted in a multiphase material. All three compounds were

determined to have a tolerance factor around 1, indicating that they should crystallize with the perovksite structure. The X-ray diffraction patterns of $Ba_{0.85}La_{0.15}(Ti_{0.85}Cr_{0.15})O_3$ and $Ba_{0.66}La_{0.33}(Ti_{0.66}Cr_{0.33})O_3$ could be indexed using a cubic unit cell and space group Pm-3m (modeled after $SrTiO_3$). The unit cell parameter, *a*, varies from 3.98 Å for $Ba_{0.85}La_{0.15}(Ti_{0.85}Cr_{0.15})O_3$ to 3.96 Å for $Ba_{0.66}La_{0.33}(Ti_{0.66}Cr_{0.33})O_3$. As the concentration of Cr^{3+} increases, the unit cell parameter decreases. This is not expected because in a six-fold coordination environment the ionic radius of Cr^{3+} (0.615 Å) is larger than the ionic radius of Ti^{4+} (0.605 Å). As a result, the substitution of Cr^{3+} for Ti^{4+} in this compound should result in a larger unit cell. However, in addition to substituting Cr^{3+} for Ti^{4+}, La^{2+} is also being substituted for Ba^{2+}. In a 12-fold coordination environment, La^{2+} has a much smaller ionic radius (1.32 Å) than Ba^{2+} (1.60 Å) and this may be the reason why the unit cell is decreases. More detailed structural studies need to be performed to determine if there is any ordering on the A- and/or B-site.

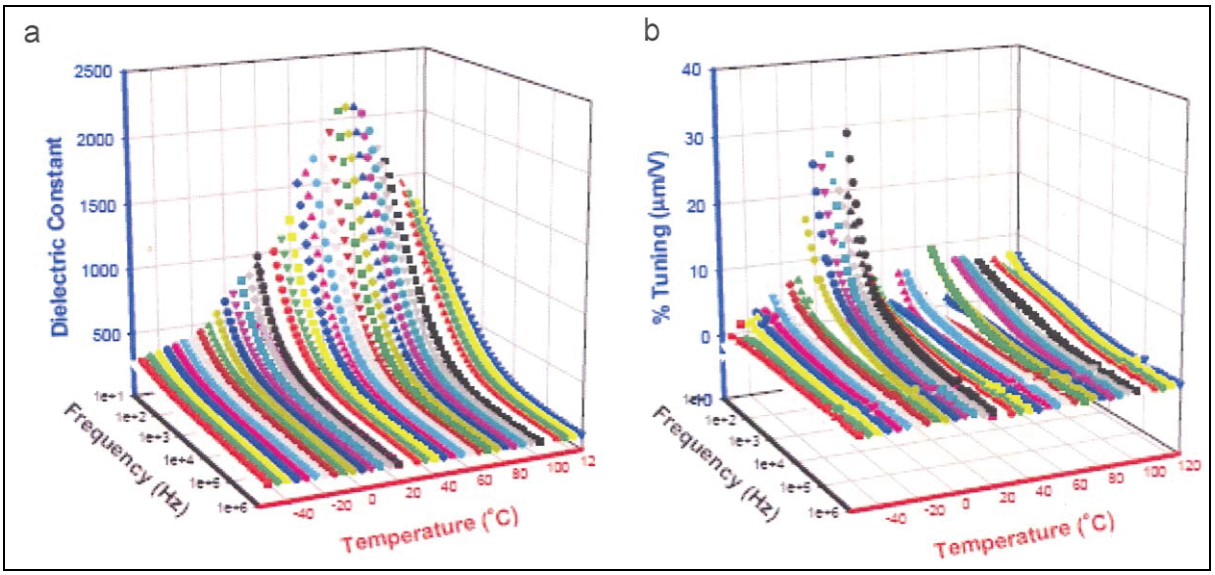

Figure 9. Dielectric constant at E=O (a) and percent tuning (b) as a function of temperature and frequency for $Ba_{0.85}La_{0.15}(Ti_{0.85}Cr_{0.15})O_3$.

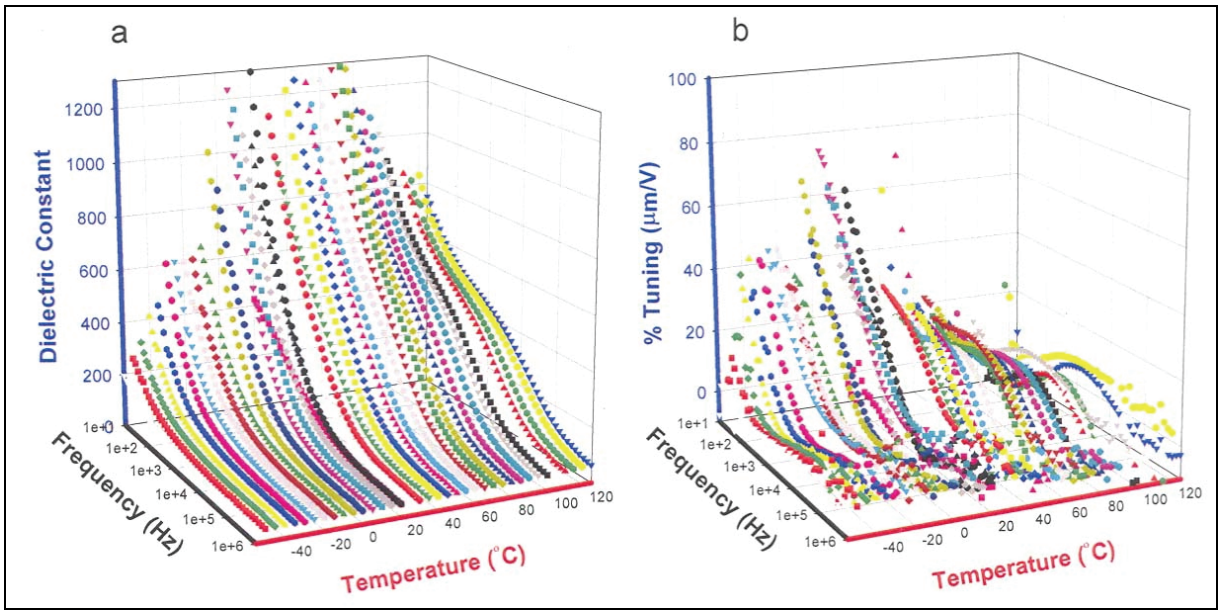

Figure 10. Dielectric constant at E=O (a) and percent tuning (b) as a function of temperature and frequency for $Ba_{0.66}La_{0.33}(Ti_{0.66}Cr_{0.33})O_3$.

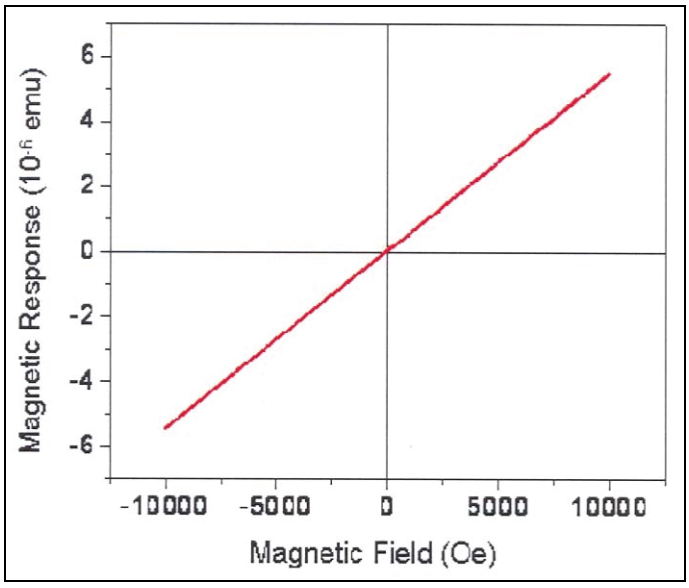

Figure 11. Magnetic response (emu) as a function of applied magnetic field (Oe) at 25 °C for $Ba_{0.66}La_{0.33}(Ti_{0.66}Cr_{0.33})O_3$ (x=0.33).

Using the Clausius-Mossotti Relation, the dielectric constant of each compound was predicted. For $Ba_{0.85}La_{0.15}(Ti_{0.85}Cr_{0.15})O_3$, a negative dielectric constant (–1200) was calculated, indicating that this compound may be on the verge of a structural phase transition that may result in ferroelectric behavior. The dielectric constants of $Ba_{0.66}La_{0.33}(Ti_{0.66}Cr_{0.33})O_3$ and $Ba_{0.33}La_{0.66}(Ti_{0.33}Cr_{0.66})O_3$ were calculated to be 640 and 40 respectively. These relatively low

positive values suggest that these materials are probably not on the verge of a structural phase transition.

For $Ba_{0.85}La_{0.15}(Ti_{0.85}Cr_{0.15})O_3$, the plot of dielectric constant versus temperature and frequency reveals a large broad peak that reaches a maximum value of ~2000 at 80 °C. This effect only occurs at frequencies less than 1 kHz. Above 1 kHz, the dielectric constant has a value of 250 and is insensitive to temperature and frequency. This compound shows less than 10% tuning over the measured temperature and frequency range. The tunability peaks sharply at ~25% around 20 °C. The reason for this sudden increase is not known.

In the case of $Ba_{0.66}La_{0.33}(Ti_{0.66}Cr_{0.33})O_3$, there is an extremely broad peak in the dielectric constant. This broad peak reaches a maximum value of 1300 at 50 °C. This only occurs at frequencies less than 10 kHz. Above 10 kHz, the dielectric constant decreases below 100 and remains insensitive to temperature and frequency. The tunability of this compound appears to fluctuation with both temperature and frequency. The tunability ranges from ~10% to almost 60% at temperatures less than 20 °C at frequencies less than 1 kHz. At higher temperatures and frequencies, the tunability decreases to less than 10%. However at 1 kHz, the tunability jumps up to ~10% at temperatures greater than 60 °C. The reason for this unusual behavior is not known at this time. Figure 11 shows the magnetic properties of this compound. At 25 °C, $Ba_{0.66}La_{0.33}(Ti_{0.66}Cr_{0.33})O_3$ does not exhibit any magnetism in the presence of an applied magnetic field ranging from –1.25 Tesla to 1.25 Tesla. This compound appears to be paramagnetic at this temperature.

Solid Solution Between $Ba_{0.66}La_{0.33}(Ti_{0.66}Fe_{0.33})O_3$ and $Ba_{0.66}La_{0.33}(Ti_{0.66}Cr_{0.33})O_3$

In the process of studying the substitution of Fe^{3+} and Cr^{3+} into the B-site of $BaTiO_3$, a solid solution was found to exist between $Ba_{0.66}La_{0.33}(Ti_{0.66}Fe_{0.33})O_3$ (rewritten as $Ba_2La(Ti_2Fe)O_9$) and $Ba_{0.66}La_{0.33}(Ti_{0.66}Cr_{0.33})O_3$ (rewritten as $Ba_2La(Ti_2Cr)O_9$). Both of these compounds were determined to have the perovskite structure, and the solid solution between them can be written as $Ba_2La[Ti_2(Fe_xCr_{1-x})]O_9$. Single phase samples with x=0, 0.25, 0.5, 0.75 and 1.0 were prepared and were also found to have the perovskite structure. Table 7 lists the tolerance factor, sample color and unit cell parameter for each of the prepared compounds. Table 8 lists the predicted dielectric constant of each compounds as well as the actual dielectric behavior. Figure 12 is the X-ray diffraction patterns of some sample within the $Ba_2La[Ti_2(Fe_xCr_{1-x})]O_9$ solid solution (x=1.0, 0.75, 0.50, 0.25 and 0.0). A plot of the dielectric constant (E=0) as a function of temperature and frequency for select samples is shown in figure 13.

Table 7. Summary of $Ba_2La[Ti_2(Fe_xCr_{1-x})]O_9$ compounds.

Compound	Tolerance Factor	Sample Color	Predicted *a* (Å)	Actual *a* (Å)	Polarizability (Å^3)	Actual Molar Volume (Å^3)
x=1.0	1.03	dark brown	4.04	3.97	15.036	65.94
x=0.75	1.03	light brown	4.05	3.97	14.967	66.43
x=0.50	1.03	brown	4.05	3.96	14.897	66.43
x=0.25	1.03	brown	4.06	3.96	14.826	66.92
x=0.0	1.02	dark yellow	4.06	3.95	14.756	66.92

Table 8. Dielectric properties of the $Ba_2La[Ti_2(Fe_xCr_{1-x})]O_9$ compounds.

Compound	Predicted Dielectric Constant *(e)*	Measured Dielectric Properties
x=1.0	–450	broad increase in e with a maximum value of 30,000 at 80 °C
x=0.75	–1500	not measured
x=0.50	–600	one small peak with a maximum value of 400 at 20 °C and a second larger peak with a maximum value of 800 at 70 °C.
x=0.25	–62000	one small peak with a maximum value of 1250 at 20 °C and a second larger peak with a maximum value of 2500 at 65 °C.
x=0.0	640	extremely broad peak in e with a maximum value of 1300 at 50 °C

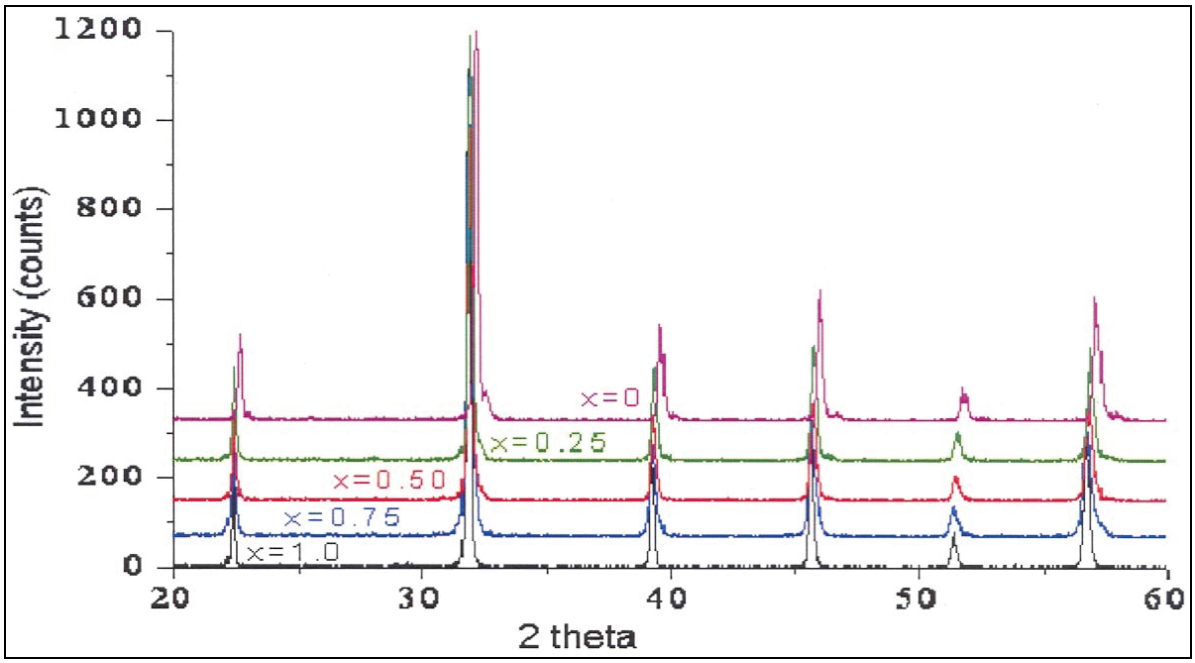

Figure 12. X-ray diffraction data for the $Ba_2La[Ti_2(Fe_xCr_{1-x})]O_9$ compounds where x=1.0, 0.75, 0.5, 0.25 and 0.0.

Various compounds within the $Ba_2La[Ti_2(Fe_xCr_{1-x})]O_9$ solid solution were successfully prepared as single phase compounds. The color ranges from dark brown for the x=l compound to dark yellow for the x=0 compound. All of these materials were determined to have a tolerance factor around 1, suggesting that they should crystallize with the perovskite structure. The fact that both

end members of this solid solution, $Ba_2La(Ti_2Fe)0_9$ and $Ba_2La(Ti_2Cr)0_9$, have the perovskite structure also indicates that all additional members of this solid solution will have the perovskite structure. The X-ray diffraction patterns of the prepared compounds could be indexed using a cubic unit cell and space group Pm-3m (modeled after $SrTiO_3$). The cubic unit cell parameter, *a*, varies from 3.97 Å for $Ba_2La(Ti_2Fe)O_9$ (x=1) to 3.95 Å for $Ba_2La(Ti_2(Cr)O_9$ for (x=0). Interestingly, the unit cell parameter decreases as the concentration of Cr^{3+} increases. Since the ionic radius of Cr^{3+} (0.615 Å) is larger than that of Fe^{3+} (0.55 Å for the low spin state), the unit cell is expected to increases as the concentration of Cr^{3+} increases. This does not occur and the reason for this is not known. More detailed structural studies need to be performed to determine why the unit cell decreases with an increasing substitution of Cr^{3+}.

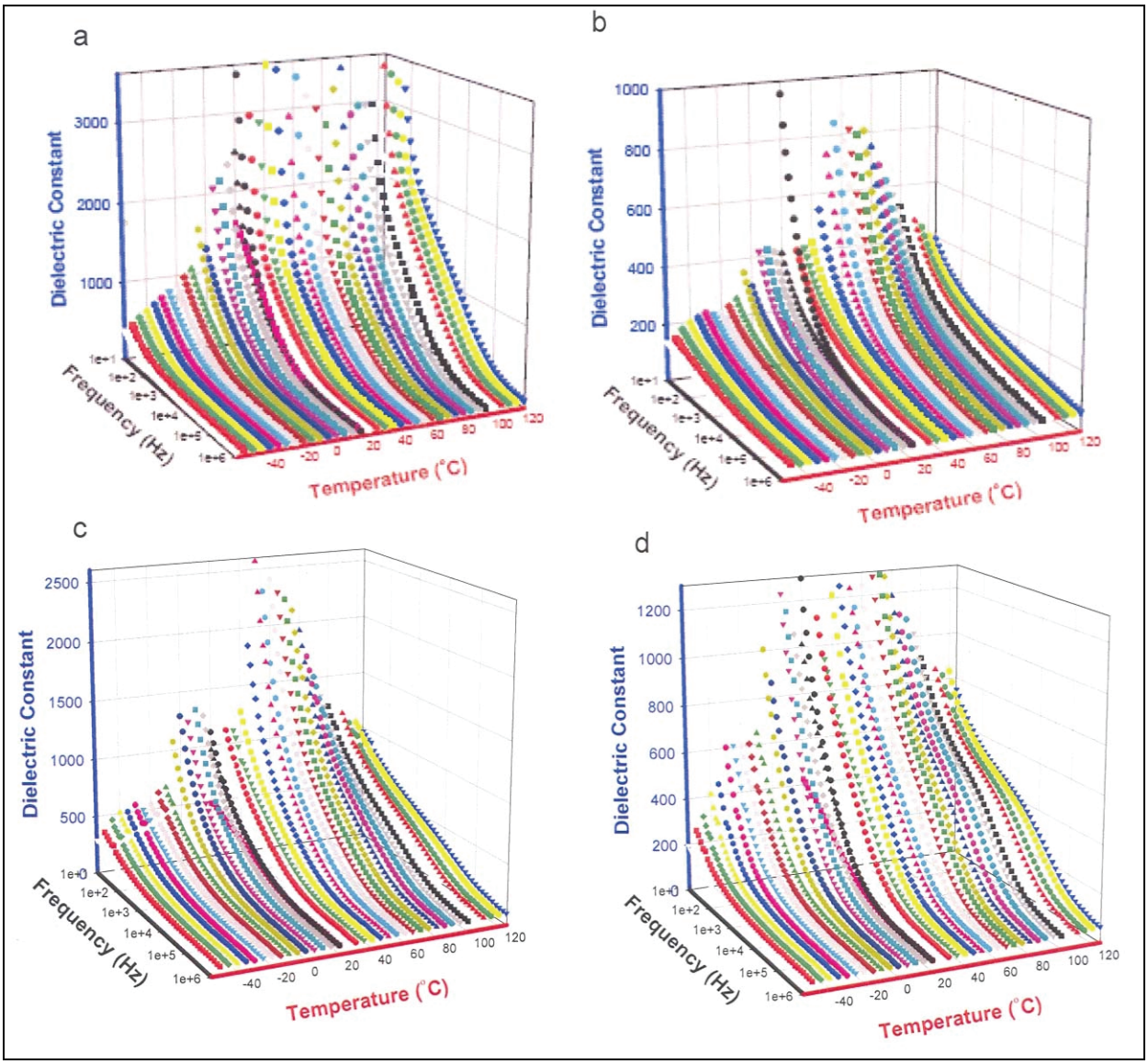

Figure 13. Dielectric constant at E=0 as a function of temperature and frequency for select samples in the $Ba_2La[Ti_2(Fe_xCr_{1-x})]O_9$ solid solution where x=1.0 (a), x=0.5 (b), x=0.25 (c) and x=0.0 (d).

Using the Clausius-Mossotti Relation, the dielectric constant of each compound was predicted. A negative dielectric constant was calculated for all members of the solid solution except for the x=0 compound. As mentioned before, these results suggest that these materials may be on the verge of a structural phase transition that may lead to ferroelectric properties. The dielectric constant of the x=0 compound was calculated to be 640, indicating that this material is probably not ferroelectric.

Figure 13 illustrates the dielectric properties of the x=1.0, 0.5, 0.25 and 0.0 members of the $Ba_2La[Ti_2(Fe_xCr_{1-x})]O_9$ solid solution. The dielectric constant of the x=1.0 compound has a very broad peak from 20 °C to 120 °C that reaches a maximum value of 30,000 (not shown in figure 13) at approximately 80 °C. This behavior is only seen at very low frequencies (less than 1 kHz). There are two peaks, one small peak and one larger peak, in the dielectric constant of the x=0.5 compound. The first (small) peak reaches a maximum value of 400 at ~20 °C and the second (larger) peak reaches a maximum value of 800 at ~70 °C. This behavior is only seen at frequencies less than 1 kHz. At all other temperatures, the dielectric constant is between 200 and 400. These two peaks are also present in the dielectric constant of the x=0.25 compound but in this material, the peaks are more well-defined. The first (small) peak reaches a maximum value of 1250 at ~20 °C and the second (larger) peak reaches a maximum value of 2500 at ~65 °C. Similar to the x=0.5 compound, this behavior is only seen at frequencies less than 1 kHz. At all other temperatures, the dielectric constant remains between 500 and 1000. Finally, for the x=1 compound, there is an extremely broad (single) peak in the dielectric constant. This broad peak reaches a maximum value of 1300 at 50°C (not shown in figure 13). The reason for the variation in the dielectric properties of this solid solution may be attributed to the interaction of the Fe^{3+} and Cr^{3+} ions. Two peaks in the dielectric constant are present for compounds that contain both Fe^{3+} and Cr^{3+}, but are not present for compounds that only contain Cr^{3+} or Fe^{3+}. More detailed studies of this solid solution need to be performed to elicit the exact cause of these results.

Since the two end members of this solid solution, $Ba_2La(Ti_2Fe)O_9$ and $Ba_2La(Ti_2Cr)O_9$, did not exhibit any magnetism at 25 °C, the magnetic properties of this solution solid were not investigated.

Substitution of (FeCr) and (FeMn) Pairs into $BaTiO_3$

Several additional materials were prepared in which pairs of magnetic atoms, such as Fe^{3+} and Cr^{3+} or Fe^{3+} and Mn^{3+}, were substituted for Ti^{4+} in $BaTiO_3$. To ensure charge neutrality, La^{3+} was substituted for Ba^{2+} on the A-site. The goal of this approach was to introduce ferrimagnetism into the material. Ferrimagnetism is a type of magnetism that occurs when a material possess two or more different magnetic sublattices. In most cases, the magnetic moments on the different sublattices align anti-parallel to each other. This results in antiferromagnetic ordering. However, if the magnitudes of the magnetic moments on each of the different sublattices are unequal, then a spontaneous magnetic moment will arise. In this

experiment, two different magnetic atoms (such as Fe^{3+} paired with Cr^{3+}) were simultaneously substituted for Ti^{4+} in $BaTiO_3$ in hopes that they would align antiferromagnetically but the difference in magnitude of their magnetic moments would result in an overall magnetic moment. Using this approach, materials with the compositions $Ba_{0.8}La_{0.2}[Ti_{0.8}(FeCr)_{0.1}]O_3$, $Ba_{0.6}La_{0.4}[Ti_{0.6}(FeCr)_{0.2}]O_3$, and $Ba_{0.8}La_{0.2}[Ti_{0.8}(Fe\ Mn)_{0.1}]O_3$ were successfully prepared. Table 9 lists the tolerance factor, sample color and unit cell parameter for each of the prepared compounds. Table 10 lists the predicted dielectric constant of each compound as well as the actual dielectric behavior. Figure 14 is the X-ray diffraction pattern of $Ba_{0.8}La_{0.2}[Ti_{0.8}(FeCr)_{0.1}]O_3$. Figure 15 is the X-ray diffraction pattern of $Ba_{0.8}La_{0.2}[Ti_{0.8}(FeMn)_{0.1}]O_3$. Figures 16 and 17 are plots of the dielectric constant (at E=O) and percent tuning as a function of temperature and frequency for $Ba_{0.8}La_{0.2}[Ti_{0.8}(FeCr)_{0.1}O_3$ and $Ba_{0.8}La_{0.2}[Ti_{0.8}(FeMn)_{0.1}]O_3$ respectively. Figure 18 is a plot of the magnetic response (emu) as a function of applied magnetic field (Oe) for $Ba_{0.8}La_{0.2}[Ti_{0.8}(FeCr)_{0.1}]O_3$ at 25 °C.

Table 9. Summary of compounds prepared by substituting (FeCr) and (FeMn) pairs into $BaTiO_3$.

Compound	**Tolerance Factor**	**Sample Color**	**Predicted *a* (Å)**	**Actual *a* (Å)**	**Polarizability (Å^3)**	**Actual Molar Volume (Å^3)**
$Ba_{0.8}La_{0.2}[Ti_{0.8}(FeCr)_{0.1}]O_3$	1.04	orange	4.08	3.97	15.082	62.57
$Ba_{0.6}La_{0.4}[Ti_{0.6}(FeCr)_{0.2}]O_3$	1.02	brown	4.04	3.96	14.804	62.099
$Ba_{0.8}La_{0.2}[Ti_{0.8}(FeMn)_{0.1}]O_3$	1.04	dark grey	4.08	3.98	15.201	6304

Table 10. Dielectric properties of compounds prepared by substituting (FeCr) and (FeMn) pairs into $BaTiO_3$.

Compound	**Predicted Dielectric Constant (ε)**	**Measured Dielectric Properties**
$Ba_{0.8}La_{0.2}[Ti_{0.8}(FeCr)_{0.1}]O_3$	–300	2 noticeable peaks: one reaches a maximum value of 500 at 30 °C and the second reaches a maximum value of 600 at 80 °C
$Ba_{0.6}La_{0.4}[Ti_{0.6}(FeCr)_{0.2}]O_3$	2000	not measured
$Ba_{0.8}La_{0.2}[Ti_{0.8}(FeMn)_{0.1}]O_3$	–300	ε steadily increases at temperatures up to and beyond 120 °C (at 120 °C, ε has a value of 325)

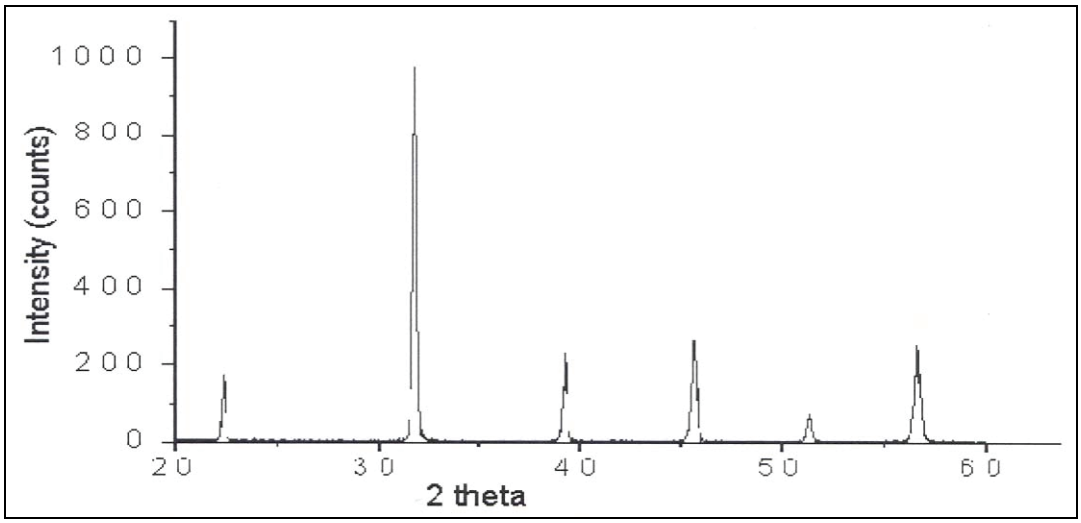

Figure 14. X-Ray diffraction pattern of $Ba_{0.8}La_{0.2}[Ti_{0.8}(FeCr)_{0.1}]O_3$.

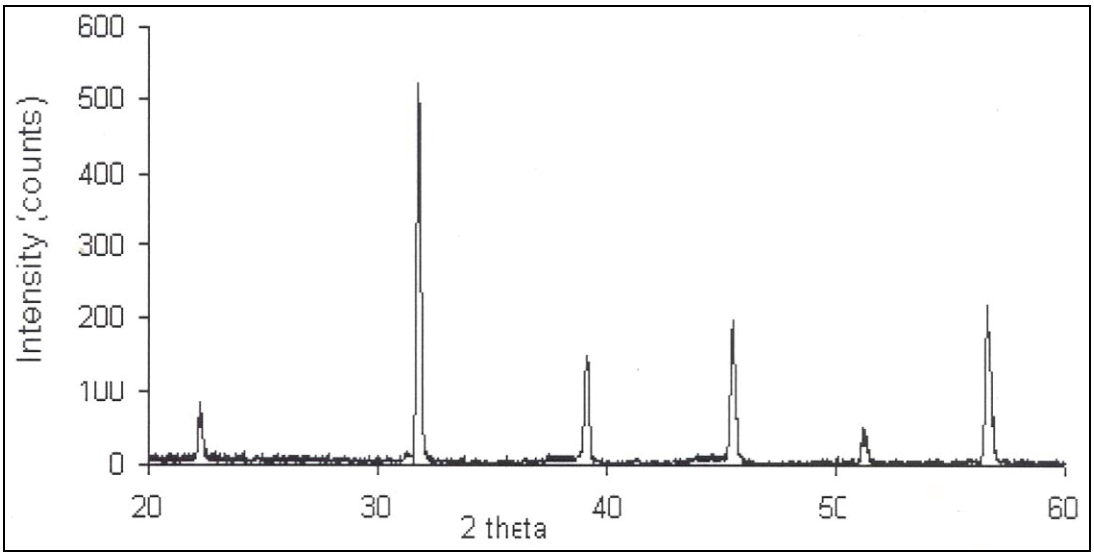

Figure 15. X-Ray Diffraction pattern of $Ba_{0.8}La_{0.2}[Ti_{0.8}(FeMn)_{0.1}]O_3$.

All three of the compounds listed in table 9 were successfully prepared as single phase compounds. The compounds range in color from orange for $Ba_{0.8}La_{0.2}[Ti_{0.8}(FeCr)_{0.1}]O_3$ to brown for $Ba_{0.6}La_{0.4}[Ti_{0.6}(FeCr)_{0.2}]O_3$ to dark grey for $Ba_{0.8}La_{0.2}[Ti_{0.8}(FeMn)_{0.1}]O_3$. The tolerance factor was determined to be around 1, indicating that these materials should crystallize with the perovskite structure. The X-ray diffraction patterns could be indexed using a cubic unit cell and space group Pm-3m (modeled after $SrTiO_3$). The cubic unit cell parameter, *a*, was found to be nearly identical for all three compounds. More detailed structural studies need to be performed to determine if there is any ordering on the A- and/or B-site.

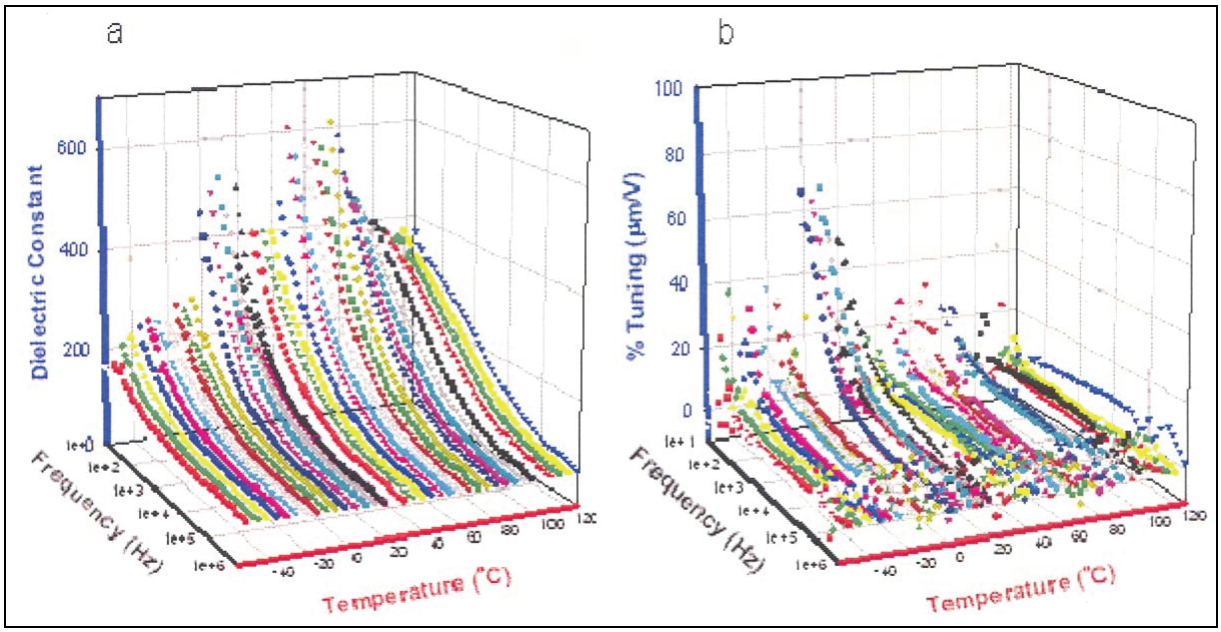

Figure 16. Dielectric constant at E=O (a) and percent tuning (b) as a function of temperature and frequency for $Ba_{0.8}La_{0.2}[Ti_{0.8}(FeCr)_{0.1}]O_3$.

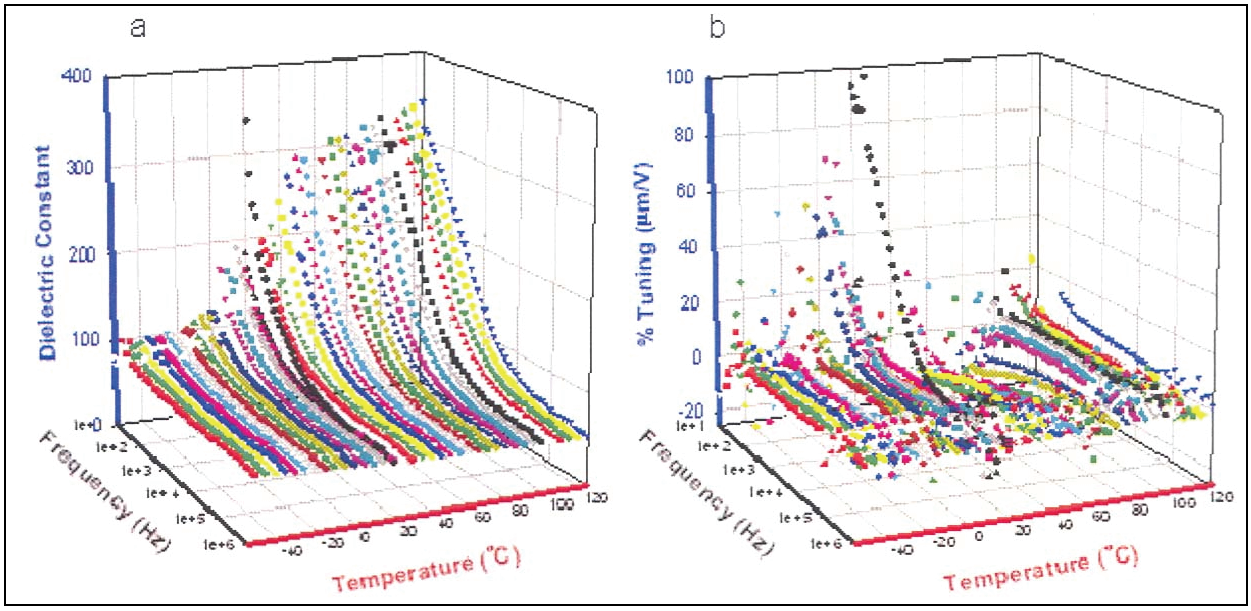

Figure 17. Dielectric constant at E=O (a) and percent tuning (b) as a function of temperature and frequency for $Ba_{0.8}La_{0.2}[Ti_{0.8}(FeMn)_{0.1}]O_3$.

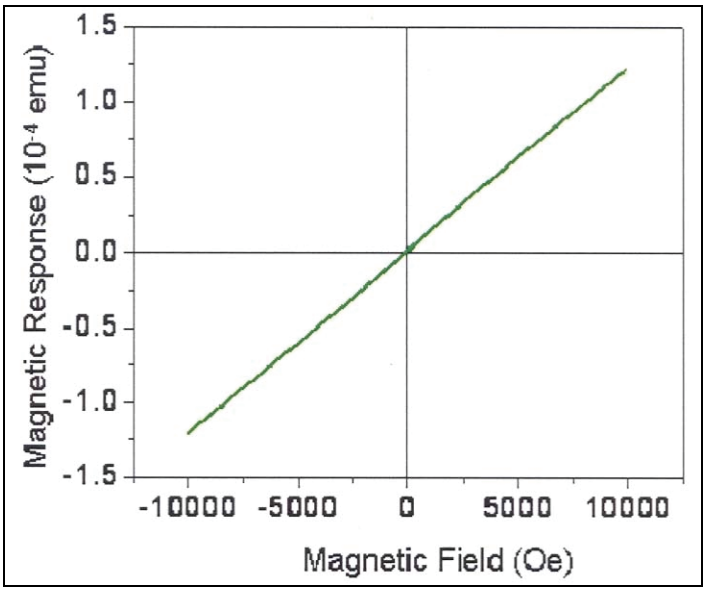

Figure 18. Magnetic response (emu) as a function of applied magnetic field (Oe) at 25 °C for $Ba_{0.8}La_{0.2}[Ti_{0.8}(FeCr)_{0.1}]O_3$.

Using the Clausius-Mossotti Relation, the dielectric constant of each compound was predicted. For $Ba_{0.8}La_{0.2}[Ti_{0.8}(FeCr)_{0.1}]O_3$ and $Ba_{0.8}La_{0.2}[Ti_{0.8}(FeMn)_{0.1}]O_3$, a negative dielectric constant (–300) was calculated. This result indicates that these two materials may be on the verge of a structural phase transition that may result in ferroelectric behavior. The dielectric constant of $Ba_{0.6}La_{0.4}[Ti_{0.6}(FeCr)_{0.2}]O_3$ was calculated to be 2000. This very large positive value suggests that this compound may also be on the verge of a structural phase transition that may result in ferroelectric behavior. However, the dielectric properties of this compound were not measured.

There are two noticeable peaks in a plot of the dielectric constant versus temperature and frequency for the $Ba_{0.8}La_{0.2}[Ti_{0.8}(FeCr)_{0.1}]O_3$ compound. These peaks are not very sharp, indicating that the material is probably not ferroelectric, but they are well-defined. The first peak reaches a maximum value of ~500 at 30 °C and the second peak reaches a maximum value of ~600 at 80 °C. The cause of these peaks is not known, but they may be the result of an interaction between the Fe^{3+} and Cr^{3+} ions. A similar result was also seen in the $Ba_2La[Ti_2(Fe_xCr_{1-x})]O_9$ solid solution. At the remaining temperatures, the dielectric constant maintains a value between 200 and 400. This effect is only present at frequencies less than 1 kHz. At higher frequencies, the dielectric constant drops below 100 and is temperature and frequency insensitive. The tunability of this compound remains fairly constant at ~10%. The sharp increase in tunability at 20 °C is most likely a result of instrument error. Figure 18 reveals the magnetic properties of $Ba_{0.8}La_{0.2}[Ti_{0.8}(FeCr)_{0.1}]O_3$. At 25 °C, this material does not exhibit any magnetism in the presence of an applied magnetic field ranging from –1.25 Tesla to 1.25 Tesla. This compound appears to be paramagnetic at this temperature.

The dielectric properties of $Ba_{0.8}La_{0.2}[Ti_{0.8}(FeMn)_{0.1}]O_3$ are quite different from those of $Ba_{0.8}La_{0.2}[Ti_{0.8}(FeCr)_{0.1}]O_3$. In this compound, the dielectric constant remains fairly stable at 100 at temperatures below 20 °C. At 20 °C, the dielectric constant starts to increase slowly. By 120 °C, the dielectric constant reaches a value of 325, but it is still increasing. It is probable that the dielectric constant will reach a maximum value at a temperature much greater than 120 °C. Similar to $Ba_{0.8}La_{0.2}[Ti_{0.8}(FeCr)_{0.1}]O_3$, this effect is only present at frequencies less than 1 kHz. At higher frequencies, the dielectric constant drops well below 100 and is temperature and frequency insensitive. This compound also exhibits almost no tunability over the measured temperature and frequency range. The sharp increase in tunability at 20 °C is most likely a result of instrument error. The magnetic properties of this compound were not investigated.

Additional Results

Attempts were also made to induce structural distortions in these compounds by varying the lanthanide (Ln^{3+}) atom on the A-site. As a result, materials were prepared with Nd^{3+} in place of La^{3+} in select compounds. Some of these compounds could be prepared as single phase materials and are listed in table 1. These compounds were found to be conducting, rather than insulating, and so further attempts to modify the A-site with other lanthanides (such as Gd^{3+} and Lu^{3+}) were not pursued.

Several single phase samples, including Ba_2CoNbO_6, Ba_2CoTaO_6 and $La_2BaMn_2\ TiO_9$, were found to be semiconducting rather than insulating and as a result, dielectric measurements could not be performed on these materials.

4. Conclusions

Many novel transition metal oxides with the perovskite structure have been successfully synthesized. These materials are based on $BaTiO_3$, in which a magnetic atom, such as Fe^{3+} or Cr^{3+}, is substituted for Ti^{4+} in an attempt to induce magnetism into the compound without destroying its ferroelectric properties. Several compounds with the compositions $Ba_{1-x}La_x(Ti_{1-x}Fe_x)O_3$ (where x=0.15, 0.33 and 0.66) and $Ba_{1-x}La_x(Ti_{1-x}Cr_x)O_3$ (where x=0.15 and 0.33) were prepared in bulk polycrystalline form. The crystal structure and the magnetic and dielectric properties of these materials were also studied. All of these compounds were found to have a cubic perovskite structure and many exhibit unique dielectric properties. Although none of the compounds is a true ferroelectric, $Ba_{0.33}La_{0.66}(Ti_{0.33}Fe_{0.66})O_3$ was found to be slightly magnetic at 25 °C. The magnetic measurements performed on this compound indicate that it is a ferromagnet.

A solid solution was found to exist between the cubic perovskite oxides $Ba_{0.66}La_{0.33}(Ti_{0.66}Fe_{0.33})O_3$ and $Ba_{0.66}La_{0.33}(Ti_{0.66}Cr_{0.33})O_3$. This solid solution can be written as $Ba_2La[Ti_2(Fe_xCr_{1-x})]O_9$, and compounds with x=0, 0.25, 0.5, 0.75 and 1.0 were successfully

prepared as single phase materials. The dielectric properties of these compounds were also studied. Although none of these materials appeared to be magnetic or ferroelectric, they did exhibit some interesting dielectric properties at low frequencies.

Attempts were also made to prepare materials in which two different magnetic atoms, such as (FeCr) and (FeMn) pairs, were substituted onto the B-site of $BaTiO_3$. The intent of this experiment was to introduce two different magnetic sublattices that would order anitferromagnetically, but the difference in the magnitude of their magnetic moments would result in a spontaneous magnetization. In essence, the material would be ferrimagnetic, as opposed to ferromagnetic. Several compounds in which (FeCr) and (FeMn) pairs were substituted for Ti^{4+} in $BaTiO_3$ were successfully prepared as single phase, polycrystalline powders. X-ray diffraction analysis revealed that all compounds have a cubic perovskite structure. The $Ba_{0.8}La_{0.2}[Ti_{0.8}(FeCr)_{0.1}]O_3$ compound was found to have dielectric properties that were similar to those of samples within the $Ba_2La[Ti_2(Fe_xCr_{1-x})]O_9$ solid solution. These unique dielectric properties may be the result of an interaction between the Fe^{3+} and Cr^{3+} ions in the material. More detailed analyses need to be performed. The magnetic properties of $Ba_{0.8}La_{0.2}[Ti_{0.8}(FeCr)_{0.1}]O_3$ was measured but the compound did not exhibit any magnetism at 25°C.

5. References

1. Schmid, H. *Ferroelectrics* **1994**, *162*, 317.
2. Ederer, C.; Spaldin, N. *Nature* **2004**, *3*, 849.
3. Khomskii, D. I. *Journal of Magnetism and Magnetic Materials* 2006, *36*, 1.
4. Spaldin, N.; Fiebig, M. *Science* **2005**, *309*, 391.
5. Fiebig, M. *Journal of Physics D: Applied Physics* **2005**, *38*, R123.
6. Spaldin, N. *Science* **2004**, *304*, 1606.
7. Hill, N. *Annual Review of Materials Research* **2002**, *32*, 1.
8. Eerenstein, W.; et al. *Nature* **2006**, *442*, 759.
9. Teage, J. R.; et al. *Solid State Communications* **1970**, *8*, 1073.
10. Sosnovska, I.; et al. *Journal of Physics* C **1982**, *15*, 4835.
11, Ederer, C.; Spaldin, N. *Physical Review B* **2005**, *71*, 060401(R).
12. Wang, J.; et al. *Science* **2003**, *299*, 1719.
13. Van Aken, B.; et al. *Nature Materials* **2004**, *3*, 164.
14. Fiebig, M.; et al. *Nature* **2002**, *419*, 818.
15. Lee, S.; et al. *Physical Review B* **2005**, *71*, 180413(R).
16. Smolenskii, G. A.; et al. *Journal of Applied Physics* **1964**, *35* (3), 915.
17. Hill, N.; et al. *Journal of Magnetism and Magnetic Materials* **2002**, *242-245*, 976.
18. Sugawara, F.; et al. *Journal of the Physical Society of Japan* **1968**, *25*, 1553.
19. Moreira dos Santos, A.; et al. *Solid State Communications* **2002**, *122*, 49.
20. Kimura, T.; et al. *Physical Review B* **2003**, *67*, 180401(R).
21. Seshadri, R.; et al. *Chemistry of Materials* **2001**, *13*, 2892.
22. Katsufuji, T.; Takagi, H. *Physical Review B* **2001**, *64*, 054415.
23. Azuma, M.; et al. *Journal of the American Chemical Society* **2005**, *127*, 8889.
24. Hemberger, J.; et al. *Nature* **2005**, *434*, 364.

25. Hur, N.; et al. *Nature* **2004**, *429*, 392.

26. Saito, K.; Kohn, K. *Journal of Physics: Condensed Matter* **1995**, *7*, 2855.

27. Baettig, P.; et al. *Applied Physics Letters* **2005**, *86*, 012505.

28. Hill, N.; et al. *Journal of Physical Chemistry B* **2002**, *106*, 3383.

29. Zheng, H.; et al. *Science* **2004**, *303*, 661.

30. Singh, M. P.; et al. *Applied Physics Letters* **2006**, *88*, 012903.

31. Clark, G. M. *The Structures of Non-Molecular Solids* John Wiley & Sons, Ltd., 1972.

32. West, A. R. *Basic Solid State Chemistry* John Wiley & Sons, Ltd., 1999.

33. Mitchell, R. H. *Perovskites: Modern and Ancient,* Almaz Press Inc., 2002.

34. Johnsson, M.; Lemmens, P. *Crystallography and Chemistry of Perovskites*. Los Alamos National Laboratory, Preprint Archive, Condensed Matter-cond-mat/0506606, 2005.

35. Colla, E. L.; et al. *Journal of Applied Physics* **1993**, *74*, 3414.

36. Lufaso, M. *Chemistry of Materials* **2004**, *16*, 2148.

No. of Copies	Organization
1	ADMNSTR
PDF	DEFNS TECHL INFO CTR ATTN DTIC OCP (ELECTRONIC COPY) 8725 JOHN J KINGMAN RD STE 0944 FT BELVOIR VA 22060-6218
1	DARPA ATTN IXO S WELBY 3701 N FAIRFAX DR ARLINGTON VA 22203-1714
1 CD	OFC OF THE SECY OF DEFNS ATTN ODDRE (R&AT) THE PENTAGON WASHINGTON DC 20301-3080
1	US ARMY RSRCH DEV AND ENGRG CMND ARMAMENT RSRCH DEV AND ENGRG CTR ARMAMENT ENGRG AND TECHNLGY CTR ATTN AMSRD AAR AEF T J MATTS BLDG 305 ABERDEEN PROVING GROUND MD 21005-5001
1	US ARMY TRADOC BATTLE LAB INTEGRATION & TECHL DIRCTRT ATTN ATCD B 10 WHISTLER LANE FT MONROE VA 23651-5850
1	PM TIMS, PROFILER (MMS-P) AN/TMQ-52 ATTN B GRIFFIES BUILDING 563 FT MONMOUTH NJ 07703
1	US ARMY INFO SYS ENGRG CMND ATTN AMSEL IE TD F JENIA FT HUACHUCA AZ 85613-5300
1	COMMANDER US ARMY RDECOM ATTN AMSRD AMR W C MCCORKLE 5400 FOWLER RD REDSTONE ARSENAL AL 35898-5000

No. of Copies	Organization
1	US ARMY RSRCH LAB ATTN AMSRD ARL CI OK TP TECHL LIB T LANDFRIED BLDG 4600 ABERDEEN PROVING GROUND MD 21005-5066
1	US GOVERNMENT PRINT OFF DEPOSITORY RECEIVING SECTION ATTN MAIL STOP IDAD J TATE 732 NORTH CAPITOL ST NW WASHINGTON DC 20402
1	DIRECTOR US ARMY RSRCH LAB ATTN AMSRD ARL RO EV W D BACH PO BOX 12211 RESEARCH TRIANGLE PARK NC 27709
3	US ARMY RSRCH LAB ATTN AMSRD ARL CI OK PE TECHL PUB ATTN AMSRD ARL CI OK TL TECHL LIB ATTN IMNE ALC IMS MAIL & RECORDS MGMT ADELPHI MD 20783-1197

Total: 14 (1 Elec, 1 CD, 12 HC)